

Supporting Information

Targeting Large Kinase Active Site with Rigid, Bulky Octahedral Ruthenium Complexes

Jasna Maksimoska, Li Feng, Klaus Harms, Chunling Yi, Joseph Kissil, Ronen Marmorstein, and Eric Meggers

*Philipps-Universität Marburg (Marburg, Germany), University of Pennsylvania (Philadelphia, USA), and
The Wistar Institute (Philadelphia, USA)*

Content:

A.) Development of Ruthenium PAK-1 inhibitors

- A.1.) Initial screening of an organometallic library for PAK1 inhibition
- A.2.) Synthesis of the octahedral ruthenium compounds **FL172** and **FL411**
- A.3.) Identification of **FL172** from an initial library of octahedral ruthenium complexes
- A.4.) Identification of **FL411** from a library of **FL172** derivatives
- A.5.) Crystallographic data of **FL389** for the determination of the relative configurations of **FL172** and **FL411**
- A.6.) Resolution of racemic mixtures and determination of absolute configurations

B.) Kinase assays

- B.1.) Kinase assays with the protein kinases PAK1, Pim1, and GSK3
- B.2.) Selectivity of **FL172** in a panel of 264 protein kinases

C.) PAK-1 crystallography

- C.1.) PAK1 expression and purification
- C.2.) Crystallization and data collection
- C.3.) Structure determination and refinement

D.) Cell-based assays

A.) Development of Ruthenium PAK-1 Inhibitors

A.1.) Initial screening of an organometallic library for PAK1 inhibition

A library of 48 organometallic compounds was tested for PAK1 inhibition at the concentration of 10 μ M with an ATP concentration of 1 μ M (see part B for details of the kinase assay). The results are shown in the bar diagram below (Figure S1) with the corresponding molecular structures of the library members displayed in Figure S2.

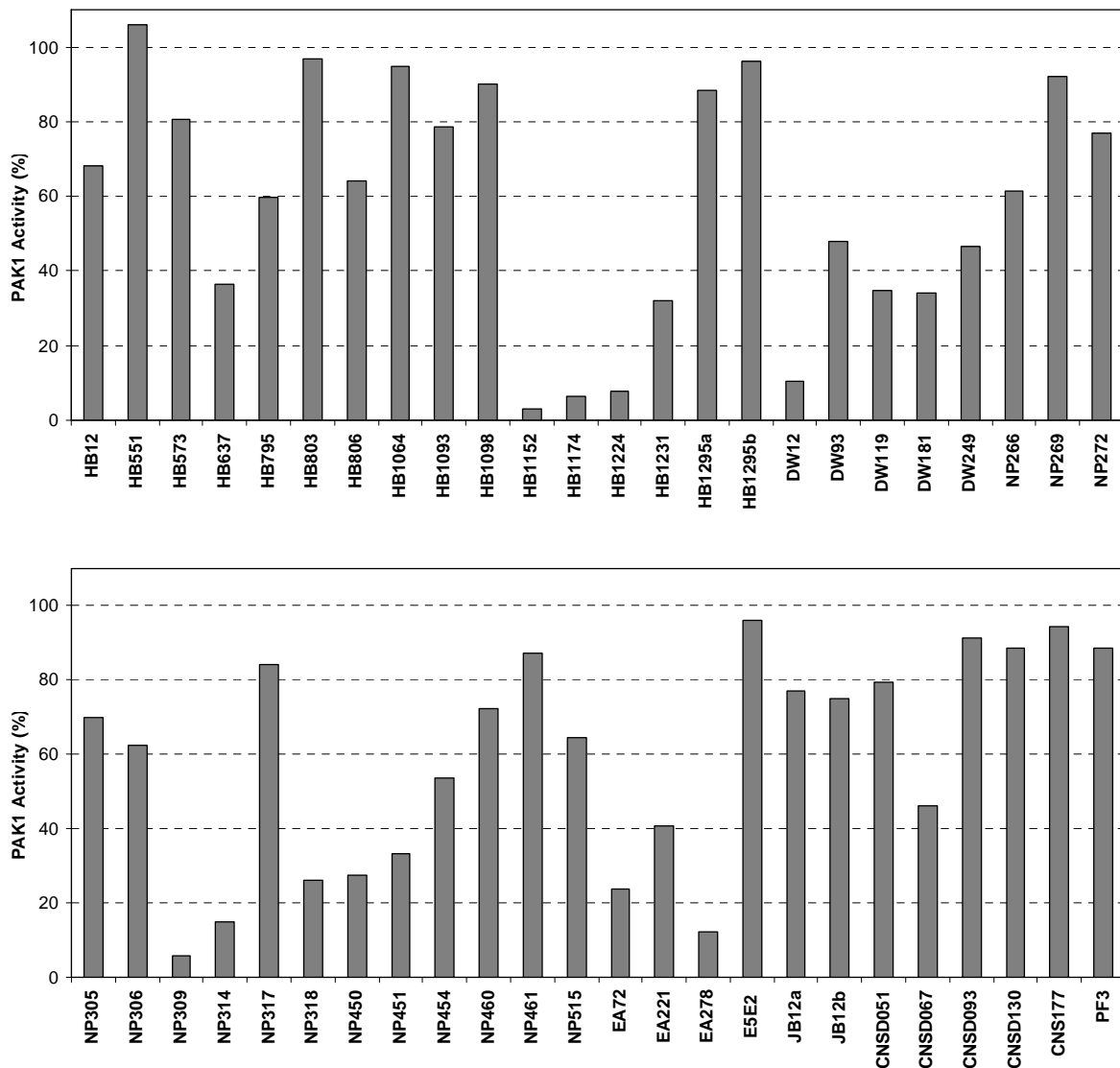
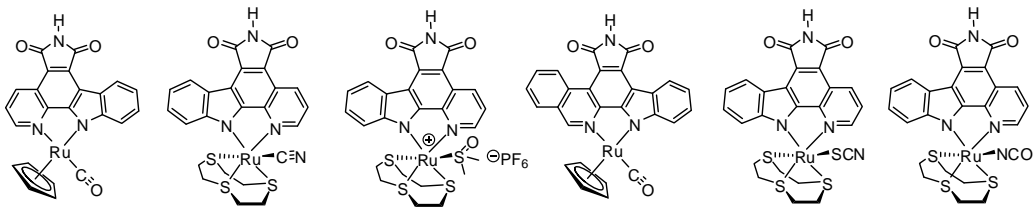
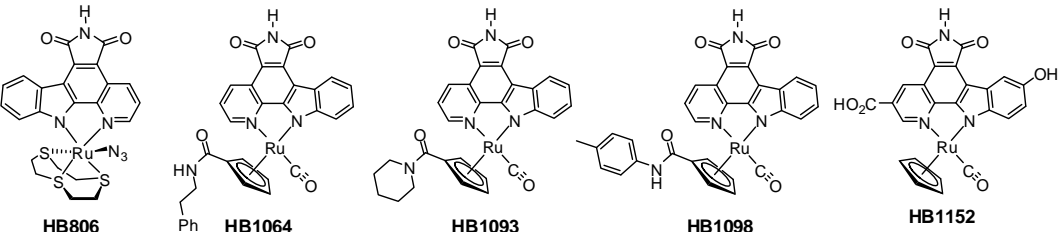


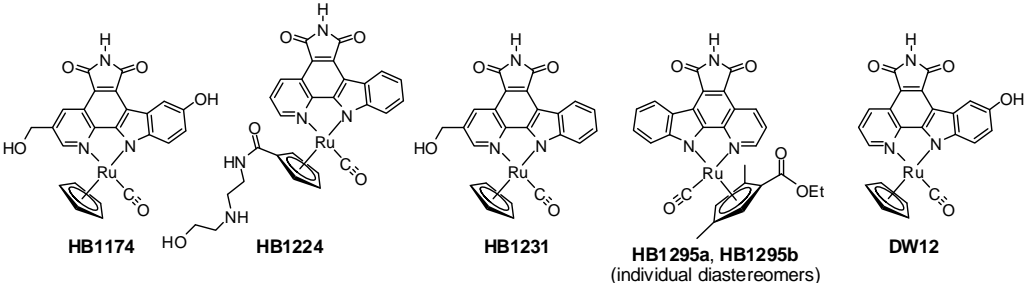
Figure S1. Initial screening of a 48-member organometallic library for PAK1 inhibition at a compound concentration of 10 μ M and 1 μ M ATP. See part B for assay details.



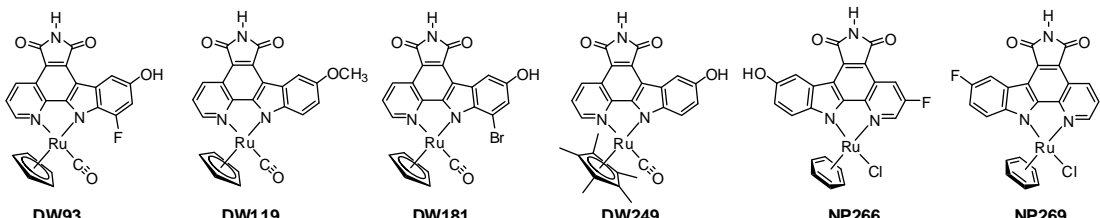
HB12 **HB551** **HB573** **HB637** **HB795** **HB803**



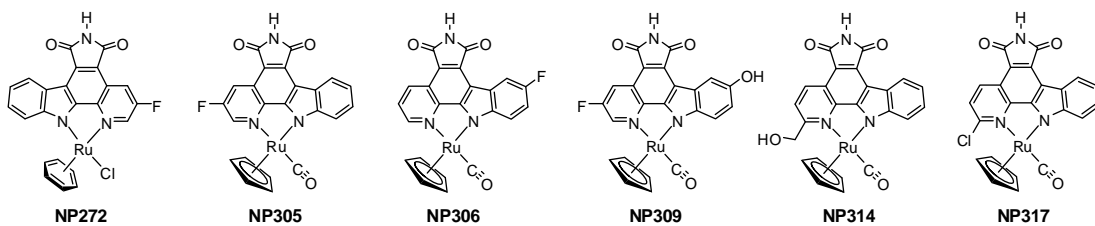
HB806 **HB1064** **HB1093** **HB1098** **HB1152**



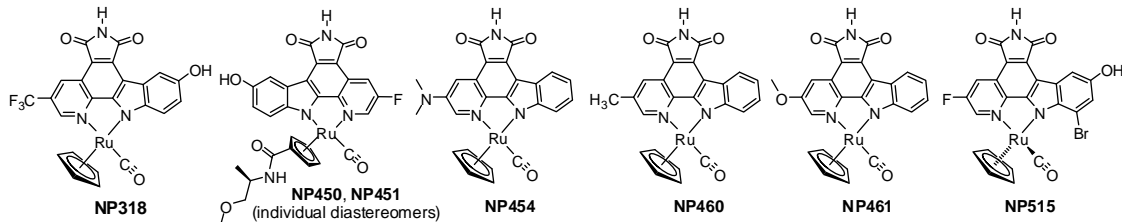
HB1295a, HB1295b
(individual diastereomers)



DW93 **DW119** **DW181** **DW249** **NP266** **NP269**



DW249 **NP272** **NP305** **NP306** **NP309** **NP314** **NP317**



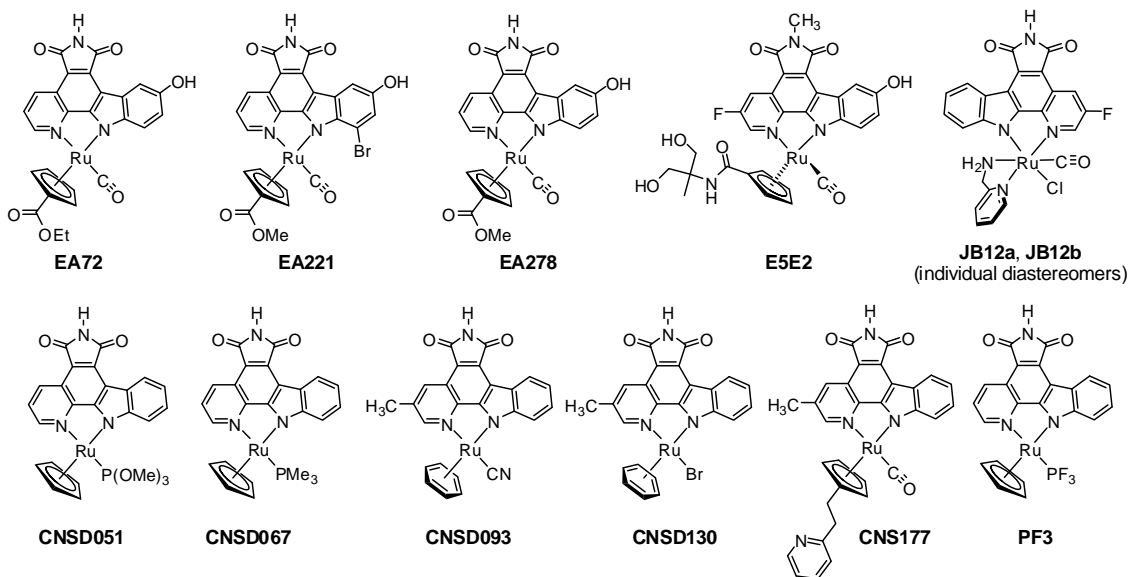


Figure S2. Molecular structures of the 48-member organometallic library. Compounds were racemic, except for **E5E2** for which the absolute stereochemistry is indicated. For the synthesis of these compounds, see: Bregman, H.; Williams, D. S.; Meggers, E. *Synthesis* **2005**, 1521-1527; Bregman, H.; Meggers, E. *Org. Lett.* **2006**, 8, 5465-5468; Atilla, G. E.; Williams, D. S.; Bregman, H.; Pagano, N.; Meggers, E. *ChemBioChem* **2006**, 7, 1443-1450; Bregman, H.; Carroll, P. J.; Meggers, E. *J. Am. Chem. Soc.* **2006**, 128, 877-884; Pagano, N.; Maksimoska, J.; Bregman, H.; Williams, D. S.; Webster, R. D.; Xue, F.; Meggers, E. *Org. Biomol. Chem.* **2007**, 5, 1218-1227. Xie, P.; Williams, D. S.; Atilla-Gokcumen, G. E.; Milk, L.; Xiao, M.; Smalley, K. S. M.; Herlyn, M.; Meggers, E.; Marmorstein, R. *ACS Chem. Biol.* **2008**, 3, 305-316.

A.2.) Synthesis of the octahedral ruthenium compounds FL172 and FL411

General Procedures. NMR spectra were recorded on a Bruker AM-400 (400 MHz) or AV-300 (300 MHz) spectrometer. Low-resolution mass spectra were obtained on an LC platform from Micromass using the ESI technique. High-resolution mass spectra were obtained on a Micromass Autospec instrument using either CI or ES ionization or a Thermo Finnigan LTQ FT instrument using either APCI or ES ionization. Infrared spectra were recorded on a Bruker IFS 88 or Perkin Elmer 1600 series FTIR spectrometer. Photolyses were performed with a medium pressure Hg lamp (150 W). Solvents and reagents were supplied from Aldrich, Acros, or Strem. Reactions were performed under an atmosphere of nitrogen unless otherwise specified. The TBS-protected pyridocarbazole **1** was synthesized as published (Pagano, N.; Maksimoska, J.; Bregman, H.; Williams, D. S.; Richard, D.; Webster, R. D.; Xue, F.; Meggers, E., *Org. Biomol. Chem.* **2007**, 5, 1218-1227). NMR standards used are as follows: (¹H NMR) CD₃CN: 1.94 ppm, (CD₃)₂CO: 2.05 ppm, DMF-*d*₇: 8.03, 2.92, 2.75 ppm. (¹³C NMR) CDCl₃: 77.23 ppm, DMSO-*d*₆: 39.51 ppm, DMF-*d*₇: 163.15, 34.89, 29.76 ppm.

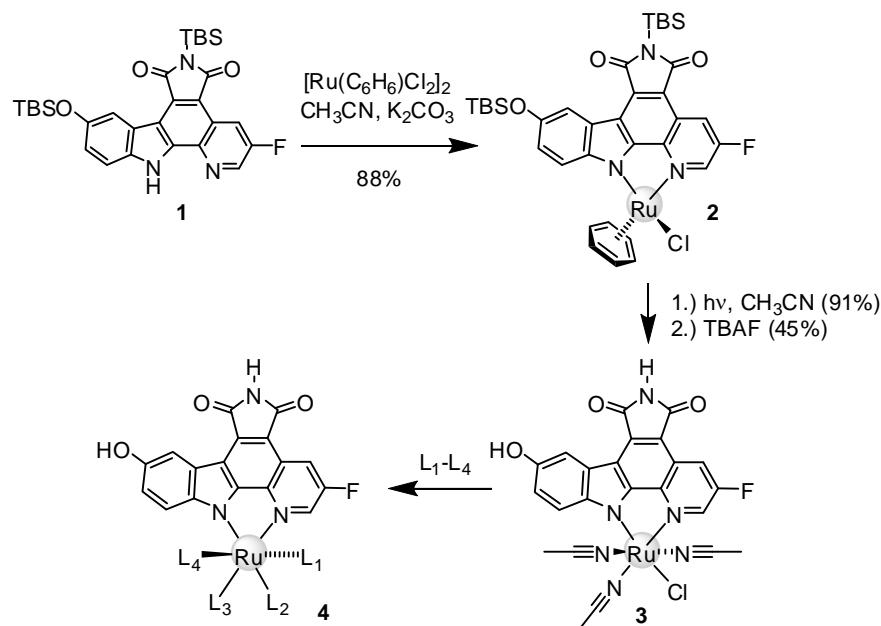


Figure S3. Synthesis of octahedral ruthenium complexes.

Compound 2. A suspension of the ligand **1** (180 mg, 0.33 mmol), K₂CO₃ (50 mg, 0.36 mmol), and [RuCl₂(η⁶-C₆H₆)]₂ (123 mg, 0.25 mmol) in CH₃CN (50 mL) was purged with nitrogen and stirred at 50 °C for 3 h. The resulting dark red suspension was dried in vacuo and the crude material was adsorbed onto silica gel and subjected to silica gel chromatography with dichloromethane : methanol (first 50:1, then 35:1) as the eluting solvent. The half-sandwich complex **2** was isolated as a dark red solid (220 mg, 88%). ¹H NMR (300 MHz, acetonitrile-*d*₃): δ (ppm) 9.46 (t, *J* = 2.6 Hz, 1H), 8.86 (dd, *J* = 9.4, 2.3 Hz, 1H), 8.25 (d, *J* = 2.5 Hz, 1H), 7.88 (d, *J* = 9.1 Hz, 1H), 7.23 (dd, *J* = 8.8, 2.6 Hz, 1H), 6.08 (s, 6H), 1.07 (s, 9H), 1.01 (s, 9H), 0.55 (s, 6H), 0.30 (s, 6H). ¹³C NMR (75.5 MHz, CDCl₃): δ (ppm) 175.1, 173.9, 157.1 (d, *J*_{C-F} = 251.4 Hz), 153.0, 150.2, 146.5, 140.9, 140.4, 140.2, 133.9, 125.0, 121.5 (d, *J*_{C-F} = 8.4 Hz), 120.7, 119.9 (d, *J*_{C-F} = 19.9 Hz), 115.0, 114.6, 113.9 (d, *J*_{C-F} = 4.9 Hz), 83.4, 26.5, 26.0, 19.1, 18.4, -4.0, -4.2. IR (film): ν (cm⁻¹) 2955, 2930, 2857, 1746, 1688, 1562, 1462, 1335, 1310, 1296, 1258, 1238, 829. HRMS calculated for C₃₅H₄₁FN₃O₃Si₂Ru (M-Cl)⁺ 728.1708, found (M-Cl)⁺ 728.1701.

Compound 3. A red solution of **2** (180 mg, 0.24 mmol) in CH₃CN (220 mL) was purged with nitrogen for 10 min and then irradiated with a mercury medium pressure lamp (pyrex filter) for 3 hours while nitrogen was bubbled through the solution. The resulting dark green solution was dried in vacuo and the crude material was adsorbed onto silica gel and subjected to silica gel chromatography with dichloromethane : methanol (first 75:1, then 35:1). The combined product eluents were isolated as a mixture of two diastereoisomers (175 mg, 91%). To the stirred green solution of the mixture (175 mg, 0.22 mmol) in CH₃CN was added tetrabutylammonium fluoride (660 μL, 1 M in THF, 0.66 mmol) at 0 °C, and the solution was stirred at 0 °C for 5 min. To the resulting green solution was added glacial acetic acid (38 μL, 0.66 mmol), and it was stirred for 2 min at 0 °C. The solution was dried in vacuo and the crude material was adsorbed onto silica gel and subjected to silica gel chromatography with

dichloromethane : methanol (first 50:1, then 20:1) to yield the precursor complex **3** (57 mg, 45%) and a second diastereoisomer in lower amounts (31 mg, 25%). Analytical data for the main diastereomer **3**: ^1H NMR (400 MHz, DMF- d_7): δ (ppm) 10.88 (s, 1H), 9.53 (t, J = 2.9 Hz, 1H), 9.27 (s, 1H), 8.65 (dd, J = 9.5, 2.5 Hz, 1H), 8.28 (d, J = 2.4 Hz, 1H), 7.81 (d, J = 8.7 Hz, 1H), 7.17 (dd, J = 8.7, 2.5 Hz, 1H), 3.04 (s, 3H), 2.27 (s, 6H). ^{13}C NMR (100.6 MHz, DMF- d_7): δ (ppm) 171.4, 171.1, 157.1 (d, $J_{\text{C}-\text{F}}$ = 246.0 Hz), 156.3, 152.2, 148.0, 144.1, 141.2, 140.9, 131.6, 127.4, 125.1, 122.8, 121.1 (d, $J_{\text{C}-\text{F}}$ = 8.5 Hz), 116.3 (d, $J_{\text{C}-\text{F}}$ = 13.6 Hz), 115.5 (d, $J_{\text{C}-\text{F}}$ = 20.6 Hz), 115.1, 110.1 (d, $J_{\text{C}-\text{F}}$ = 4.6 Hz), 109.0 (the methyl group peaks were hidden by the solvent peak). IR (film): ν (cm^{-1}) 2277, 1721, 1649, 1529, 1497, 1469, 1437, 1384, 1083, 1028, 774. HRMS calculated for $\text{C}_{23}\text{H}_{16}\text{FN}_6\text{O}_3\text{Ru}$ ($\text{M} - \text{Cl}$) $^+$ 545.0306, found ($\text{M} - \text{Cl}$) $^+$ 545.0307.

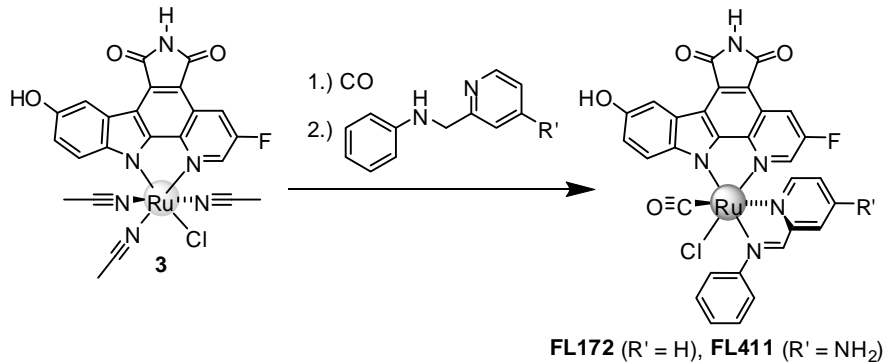


Figure S4. Synthesis of **FL172** and **FL411**.

Complex FL172. A solution of precursor complex **3** (7 mg, 0.012 mmol) in DMF (2 mL) was purged with CO gas for 5 min, then stirred at 75 °C under the atmosphere of CO for 1 hour. To the resulting solution was added 2-(phenylaminomethyl)pyridine (120 μL , 100 mM in DMF), then the solution was stirred at 95 °C under the atmosphere of nitrogen for 1.5 hours, after which the purple solution was dried under high vacuum. The crude material was adsorbed onto silica gel and subjected to silica gel chromatography with dichloromethane :

methanol (50:1) to yield compound **FL172** as a single diastereomer (3.5 mg, 44%). The relative configuration was initially determined by NOE measurements (data not shown) and later confirmed by a crystal structure of a derivative (see A.2.). ¹H NMR (300 MHz, acetone-*d*₆): δ (ppm) 9.89 (s, 1H), 9.22 (s, 1H), 8.69 (dd, *J* = 9.4, 2.4 Hz, 1H), 8.59 (d, *J* = 8.9 Hz, 1H), 8.38 (dt, *J* = 7.7, 0.9 Hz, 1H), 8.36 (t, *J* = 2.6 Hz, 1H), 8.31 (dd, *J* = 2.5, 0.4 Hz, 1H), 8.21 (s, 1H), 8.16 (td, *J* = 7.6, 1.9 Hz, 1H), 8.13 (m, 2H), 7.69 (m, 2H), 7.59 (m, 1H), 7.48 (m, 1H), 7.44 (td, *J* = 5.4, 1.3 Hz, 1H), 7.15 (dd, *J* = 8.9, 2.6 Hz, 1H). ¹³C NMR (100.6 MHz, DMSO-*d*₆): δ (ppm) 200.7, 170.4 (d, *J*_{C-F} = 16.9 Hz), 169.7, 157.6, 155.1, 154.4, 153.1, 151.8, 147.5 (d, *J*_{C-F} = 217.4 Hz), 141.3 (d, *J*_{C-F} = 33.8 Hz), 140.5, 139.7, 131.7, 129.5, 129.1 (d, *J*_{C-F} = 23.9 Hz), 128.3, 124.3, 122.4, 120.3 (d, *J*_{C-F} = 8.3 Hz), 117.9, 117.6 (d, *J*_{C-F} = 19.6 Hz), 116.5, 114.4, 111.0, 108.1. IR (film): ν (cm⁻¹) 3199, 2919, 1962, 1687, 1650, 1499, 1469, 1428, 1405, 1384, 1335, 1028. HRMS calculated for C₃₀H₁₇ClFN₅O₄RuNa (M + Na)⁺ 689.9889, found (M + Na)⁺ 689.9906.

Complex FL411. A solution of precursor complex **3** (7 mg, 0.012 mmol) in DMF (2 mL) was purged with CO gas for 5 min, then stirred at 75 °C under the atmosphere of CO for 1 hour. To the resulting solution was added 2-(phenylaminomethyl)-4-aminopyridine (120 μL, 100 mM in DMF), then the solution was stirred at 95 °C under the atmosphere of nitrogen for 3 hours, after which the purple solution was dried under high vacuum. The crude material was adsorbed onto silica gel and subjected to silica gel chromatography with dichloromethane : methanol (35:1) to obtain compound **FL411** (2.5 mg, 30%). ¹H NMR (300 MHz, acetone-*d*₆): δ (ppm) 9.86 (s, 1H), 8.90 (s, 1H), 8.70 (dd, *J* = 9.4, 2.4 Hz, 1H), 8.60 (d, *J* = 8.9 Hz, 1H), 8.32 (t, *J* = 2.6 Hz, 1H), 8.29 (d, *J* = 2.3 Hz, 1H), 8.18 (s, 1H), 8.09 (m, 2H), 7.65 (m, 2H), 7.54 (m, 1H), 7.45 (d, *J* = 2.5 Hz, 1H), 7.14 (dd, *J* = 8.9, 2.6 Hz, 1H), 6.78 (d, *J* = 6.3 Hz, 1H), 6.53 (s, 2H), 6.43 (dd, *J* = 6.3, 2.5 Hz, 1H). ¹³C NMR (100.6 MHz, DMSO-*d*₆): δ (ppm) 200.6, 170.6, 170.4 (d, *J*_{C-F} = 13.4 Hz), 157.6, 155.3 (d, *J*_{C-F} = 211.5 Hz), 155.1,

153.2 (d, $J_{C-F} = 5.3$ Hz), 151.7, 147.3, 146.5, 140.6, 140.5 (d, $J_{C-F} = 33.4$ Hz), 131.7, 129.3, 128.6, 124.1, 122.4, 120.2 (d, $J_{C-F} = 8.5$ Hz), 118.0, 117.3 (d, $J_{C-F} = 20.1$ Hz), 116.3, 114.3, 114.2, 110.6 (d, $J_{C-F} = 4.9$ Hz), 110.4, 108.0. IR (film): ν (cm⁻¹) 3312, 3204, 1960, 1715, 1470, 1454, 1385, 1335, 1099, 1024, 403. HRMS calculated for C₃₀H₁₈ClFN₆O₄RuNa (M + Na)⁺ 704.9998, found (M + Na)⁺ 704.9991.

A.3.) Identification of **FL172** from an initial library of octahedral ruthenium complexes

Reactions were executed by the reaction of precursor complex **3** with CO plus different bidentate ligands, affording complexes of type **S1** (Figure S5), in analogy to the synthesis of **FL172** and **FL411** (see part A.2).

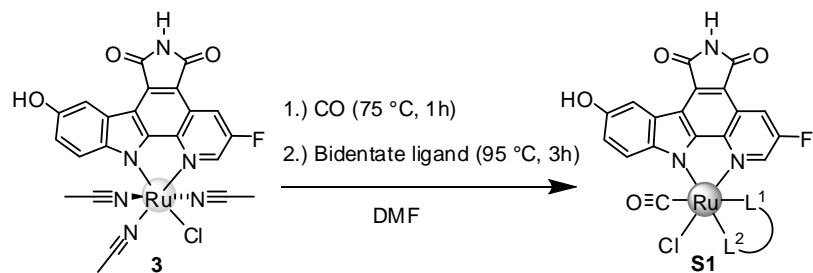


Figure S5. Bidentate ligands used for the synthesis of octahedral ruthenium complexes.

The products were purified by silica gel chromatography and the constitutions each confirmed by mass spectrometry and ¹H-NMR analysis. Relative configurations were assigned by ¹H-NMR based on the presence or absence of upfield shifted indole H-9 protons produced by the ring-current of adjacent conjugated aromatic π-systems (Figure S6), whereas **FL162-1** and **FL162-2** were assigned by their retention times during silica gel chromatography. A subset of bidentate ligands afforded mixtures of multiple isomers which could not be resolved (data not shown). Such mixtures were not considered for further studies. Figure S7 shows the molecular structures of synthesized and characterized complexes. Initial inhibitory activities were tested against PAK1 at a single concentration of 1 μM at an ATP concentration of 1 μM (Figure S8). Overall, **FL172** showed the most promising inhibitory properties (18% activity at 1 μM with 1 μM ATP).

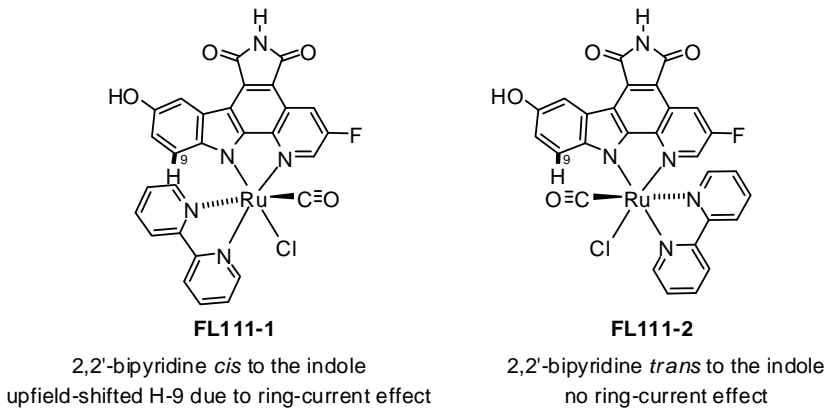


Figure S6. Example of the assignment of the relative stereochemistry of octahedral complexes in Figure S7 by ^1H -NMR spectroscopy.

Complex FL115-1. ^1H NMR (300 MHz, acetone- d_6): δ (ppm) 9.86 (s, 1H), 9.36 (d, J = 8.9 Hz, 1H), 9.20 (t, J = 2.6 Hz, 1H), 8.81 (dd, J = 9.4, 2.6 Hz, 1H), 8.20 (d, J = 2.2 Hz, 1H), 8.12 (s, 1H), 8.08 (td, J = 7.8, 1.5 Hz, 1H), 7.67 (m, 2H), 6.78 (dd, J = 8.8, 2.6 Hz, 1H), 5.96 (d, J = 8.9 Hz, 1H), 4.82 (m, 3H), 4.22 (m, 1H). HRMS calculated for $\text{C}_{24}\text{H}_{16}\text{ClFN}_5\text{O}_4\text{Ru}$ ($M + \text{H}$) $^+$ 593.9913, found ($M + \text{H}$) $^+$ 593.9949.

Complex FL115-2. ^1H NMR (300 MHz, acetone- d_6): δ (ppm) 9.82 (s, 1H), 9.25 (d, J = 5.2 Hz, 1H), 8.74 (dd, J = 9.5, 2.4 Hz, 1H), 8.45 (d, J = 8.9 Hz, 1H), 8.21 (d, J = 2.4 Hz, 1H), 8.10 (s, 1H), 8.02 (td, J = 7.7, 1.5 Hz, 1H), 7.90 (m, 1H), 7.69 (d, J = 7.8 Hz, 1H), 7.60 (m, 1H), 7.09 (dd, J = 8.9, 2.6 Hz, 1H), 4.92 (m, 3H), 4.51 (m, 1H). HRMS calculated for $\text{C}_{24}\text{H}_{16}\text{ClFN}_5\text{O}_4\text{Ru}$ ($M + \text{H}$) $^+$ 593.9913, found ($M + \text{H}$) $^+$ 593.9934.

Complex FL114-1. Formed as two diastereoisomers with the ratio of approximately 1:1. ^1H NMR (300 MHz, acetone- d_6): δ (ppm) 9.86 (s, 2H), 9.48 (m, 1H), 9.37 (m, 1H), 9.23 (t, J = 2.7 Hz, 1H), 9.17 (t, J = 2.6 Hz, 1H), 8.82 (dd, J = 9.4, 2.5 Hz, 2H), 8.20-8.08 (m, 6H), 7.69-7.65 (m, 4H), 6.78 (m, 2H), 6.07 (d, J = 8.8 Hz, 1H), 5.89 (d, J = 8.7 Hz, 1H), 5.31 (m, 2H),

5.16 (m, 1H), 4.55 (m, 1H), 4.30 (m, 2H), 1.71 (d, $J = 6.3$ Hz, 3H), 1.42 (d, $J = 7.0$ Hz, 3H).

HRMS calculated for $\text{C}_{25}\text{H}_{18}\text{ClFN}_5\text{O}_4\text{Ru}$ ($\text{M} + \text{H}$)⁺ 608.0069, found ($\text{M} + \text{H}$)⁺ 608.0057.

Complex FL114-2. Formed as two diastereomers with the ratio of approximately 1:1. ¹H NMR (300 MHz, acetone-*d*₆): δ (ppm) 9.81 (s, 2H), 9.36 (m, 1H), 9.24 (m, 1H), 8.76-8.69 (m, 2H), 8.49 (d, $J = 8.8$ Hz, 1H), 8.41 (d, $J = 8.9$ Hz, 1H), 8.21 (d, $J = 2.5$ Hz, 2H), 8.11-8.04 (m, 4H), 7.91 (t, $J = 2.5$ Hz, 1H), 7.85 (t, $J = 2.5$ Hz, 1H), 7.69-7.57 (m, 4H), 7.10 (dd, $J = 2.5, 1.5$ Hz, 1H), 7.07 (dd, $J = 2.5, 1.5$ Hz, 1H), 5.29 (m, 3H), 4.60 (m, 2H), 4.45 (m, 1H), 1.78 (d, $J = 6.6$ Hz, 3H), 1.64 (d, $J = 6.7$ Hz, 3H). HRMS calculated for $\text{C}_{25}\text{H}_{18}\text{ClFN}_5\text{O}_4\text{Ru}$ ($\text{M} + \text{H}$)⁺ 608.0069, found ($\text{M} + \text{H}$)⁺ 608.0059.

Complex FL111-1. ¹H NMR (300 MHz, acetone-*d*₆): δ (ppm) 9.88 (s, 1H), 9.79 (d, $J = 5.8$ Hz, 1H), 9.40 (t, $J = 2.8$ Hz, 1H), 8.96 (dd, $J = 9.3, 2.5$ Hz, 1H), 8.77 (d, $J = 8.1$ Hz, 1H), 8.63 (d, $J = 8.4$ Hz, 1H), 8.38 (td, $J = 8.0, 1.5$ Hz, 1H), 8.11-8.01 (m, 3H), 7.93 (m, 1H), 7.76 (d, $J = 5.5$ Hz, 1H), 7.35 (m, 1H), 6.69 (dd, $J = 8.8, 2.6$ Hz, 1H), 5.84 (d, $J = 8.8$ Hz, 1H). HRMS calculated for $\text{C}_{28}\text{H}_{15}\text{Cl}_2\text{FN}_5\text{O}_4\text{Ru}$ ($\text{M} + \text{Cl}$)⁻ 675.9529, found ($\text{M} + \text{Cl}$)⁻ 675.9471.

Complex FL111-2. ¹H NMR (300 MHz, acetone-*d*₆): δ (ppm) 9.87 (s, 1H), 9.61 (d, $J = 5.6$ Hz, 1H), 8.74 (d, $J = 7.9$ Hz, 1H), 8.68-8.64 (m, 2H), 8.55 (d, $J = 8.9$ Hz, 1H), 8.32-8.27 (m, 2H), 8.19 (s, 1H), 8.11 (td, $J = 8.1, 1.6$ Hz, 1H), 7.87 (m, 1H), 7.80 (t, $J = 2.6$ Hz, 1H), 7.52 (d, $J = 5.4$ Hz, 1H), 7.35 (m, 1H), 7.15 (dd, $J = 8.9, 2.6$ Hz, 1H). HRMS calculated for $\text{C}_{28}\text{H}_{16}\text{ClFN}_5\text{O}_4\text{Ru}$ ($\text{M} + \text{H}$)⁺ 641.9913, found ($\text{M} + \text{H}$)⁺ 641.9898.

Complex FL161-1. ¹H NMR (300 MHz, acetone-*d*₆): δ (ppm) 9.89 (s, 1H), 9.38 (t, $J = 2.6$ Hz, 1H), 8.96 (dd, $J = 9.3, 2.5$ Hz, 1H), 8.56 (t, $J = 8.3$ Hz, 2H), 8.23 (t, $J = 7.9$ Hz, 1H), 8.10-7.94 (m, 4H), 7.71 (d, $J = 5.5$ Hz, 1H), 7.31 (m, 1H), 6.70 (dd, $J = 8.8, 2.6$ Hz, 1H), 5.78 (d, $J = 8.9$ Hz, 1H), 3.46 (s, 3H). HRMS calculated for $\text{C}_{29}\text{H}_{18}\text{ClFN}_5\text{O}_4\text{Ru}$ ($\text{M} + \text{H}$)⁺ 656.0069, found ($\text{M} + \text{H}$)⁺ 656.0052.

Complex FL161-2. ^1H NMR (300 MHz, acetone- d_6): δ (ppm) 9.88 (s, 1H), 8.66-8.53 (m, 4H), 8.31 (d, J = 2.6 Hz, 1H), 8.21 (s, 1H), 8.16 (t, J = 7.9 Hz, 1H), 8.07 (td, J = 8.2, 1.7 Hz, 1H), 7.88 (d, J = 7.8 Hz, 1H), 7.71 (t, J = 2.2 Hz, 1H), 7.49 (d, J = 5.5 Hz, 1H), 7.30 (m, 1H), 7.16 (dd, J = 8.9, 2.6 Hz, 1H), 3.41 (s, 3H). HRMS calculated for $\text{C}_{29}\text{H}_{18}\text{Cl}_2\text{FN}_5\text{O}_4\text{Ru}$ ($M + \text{Cl}^-$) 689.9685, found ($M + \text{Cl}^-$) 689.9655.

Complex FL174-1. HRMS calculated for $\text{C}_{34}\text{H}_{19}\text{ClFN}_5\text{O}_4\text{Ru}$ (M) $^+$ 717.0153, found (M) $^+$ 717.0350.

Complex FL174-2. ^1H NMR (300 MHz, acetone- d_6): δ (ppm) 9.83 (s, 1H), 8.77 (dd, J = 8.2, 1.3 Hz, 1H), 8.67 (d, J = 8.2 Hz, 1H), 8.62-8.56 (m, 2H), 8.33 (t, J = 7.9 Hz, 1H), 8.26 (d, J = 2.6 Hz, 1H), 8.17 (s, 1H), 8.15-7.81 (m, 4H), 7.61-7.48 (m, 5H), 7.35 (m, 1H), 7.12 (dd, J = 8.8, 2.6 Hz, 1H). HRMS calculated for $\text{C}_{34}\text{H}_{20}\text{ClFN}_5\text{O}_4\text{Ru}$ ($M + \text{H}$) $^+$ 718.0226, found ($M + \text{H}$) $^+$ 718.0204.

Complex FL178. ^1H NMR (300 MHz, acetone- d_6): δ (ppm) 9.85 (s, 1H), 8.64-8.60 (m, 2H), 8.55 (d, J = 8.2 Hz, 1H), 8.40 (d, J = 8.0 Hz, 1H), 8.28 (d, J = 2.6 Hz, 1H), 8.19-8.14 (m, 2H), 7.87 (t, J = 7.9 Hz, 1H), 7.80 (d, J = 7.8 Hz, 1H), 7.29 (m, 1H), 7.20 (dd, J = 8.9, 2.6 Hz, 1H), 7.15 (d, J = 7.9 Hz, 1H), 3.45 (s, 3H), 1.93 (s, 3H). HRMS calculated for $\text{C}_{30}\text{H}_{20}\text{ClFN}_5\text{O}_4\text{Ru}$ ($M + \text{H}$) $^+$ 670.0226, found ($M + \text{H}$) $^+$ 670.0225.

Complex FL134. ^1H NMR (300 MHz, acetone- d_6): δ (ppm) 9.87 (s, 1H), 9.41 (s, 1H), 8.65 (dd, J = 9.5, 2.4 Hz, 1H), 8.55 (d, J = 8.7 Hz, 2H), 8.48 (d, J = 8.3 Hz, 1H), 8.32 (d, J = 2.6 Hz, 1H), 8.18 (s, 1H), 8.08 (d, J = 8.3 Hz, 1H), 7.89 (d, J = 8.4 Hz, 1H), 7.77 (t, J = 2.5 Hz, 1H), 7.36 (m, 1H), 7.15 (dd, J = 8.9, 2.6 Hz, 1H), 2.64 (s, 3H), 1.92 (s, 3H). HRMS calculated for $\text{C}_{30}\text{H}_{20}\text{ClFN}_5\text{O}_4\text{Ru}$ ($M + \text{H}$) $^+$ 670.0226, found ($M + \text{H}$) $^+$ 670.0203.

Complex FL151-1. ^1H NMR (300 MHz, DMSO- d_6): δ (ppm) 11.13 (s, 1H), 10.05 (dd, J = 5.3, 1.1 Hz, 1H), 9.27 (t, J = 2.6 Hz, 1H), 9.04 (s, 1H), 9.00 (dd, J = 8.3, 1.1 Hz, 1H), 8.95 (dd, J = 9.2, 2.5 Hz, 1H), 8.74 (dd, J = 8.3, 1.2 Hz, 1H), 8.40-8.22 (m, 3H), 8.01 (dd, J = 5.1, 1.2 Hz, 1H), 7.88 (d, J = 2.4 Hz, 1H), 7.71 (dd, J = 8.2, 5.1 Hz, 1H), 6.40 (dd, J = 8.8, 2.5 Hz, 1H), 5.31 (d, J = 8.8 Hz, 1H). HRMS calculated for $\text{C}_{30}\text{H}_{16}\text{ClFN}_5\text{O}_4\text{Ru}$ ($M + H$) $^+$ 665.9913, found ($M + H$) $^+$ 665.9923.

Complex FL151-2. ^1H NMR (300 MHz, acetone- d_6): δ (ppm) 9.97 (dd, J = 5.2, 1.3 Hz, 1H), 9.89 (s, 1H), 8.91 (dd, J = 8.3, 1.3 Hz, 1H), 8.73 (dd, J = 8.2, 1.4 Hz, 1H), 8.63-8.59 (m, 2H), 8.38-8.21 (m, 5H), 7.83 (dd, J = 5.1, 1.5 Hz, 1H), 7.77-7.70 (m, 2H), 7.17 (dd, J = 8.8, 2.6 Hz, 1H). HRMS calculated for $\text{C}_{30}\text{H}_{16}\text{ClFN}_5\text{O}_4\text{Ru}$ ($M + H$) $^+$ 665.9913, found ($M + H$) $^+$ 665.9906.

Complex FL182-1. ^1H NMR (300 MHz, acetone- d_6): δ (ppm) 9.89 (s, 1H), 9.74 (m, 1H), 9.31 (t, J = 2.6 Hz, 1H), 8.90 (dd, J = 9.3, 2.6 Hz, 1H), 8.39 (td, J = 7.8, 1.4 Hz, 1H), 8.21-8.17 (m, 2H), 8.11 (s, 1H), 8.06 (m, 1H), 6.74 (dd, J = 8.8, 2.6 Hz, 1H), 5.92 (d, J = 8.8 Hz, 1H), 4.92 (m, 1H), 4.68 (m, 1H), 3.89 (m, 1H), 3.17 (m, 1H). HRMS calculated for $\text{C}_{26}\text{H}_{16}\text{ClFN}_5\text{O}_5\text{Ru}$ ($M + H$) $^+$ 633.9862, found ($M + H$) $^+$ 633.9844.

Complex FL182-2. ^1H NMR (300 MHz, acetone- d_6): δ (ppm) 9.85 (s, 1H), 9.53 (m, 1H), 8.71 (dd, J = 9.5, 2.4 Hz, 1H), 8.51 (d, J = 8.9 Hz, 1H), 8.31 (td, J = 7.8, 1.4 Hz, 1H), 8.25 (d, J = 2.6 Hz, 1H), 8.16 (m, 1H), 8.12 (s, 1H), 7.97 (m, 1H), 7.93 (t, J = 2.5 Hz, 1H), 7.11 (dd, J = 8.9, 2.6 Hz, 1H), 4.91 (m, 1H), 4.64 (m, 1H), 3.66 (m, 1H), 3.12 (m, 1H). HRMS calculated for $\text{C}_{26}\text{H}_{16}\text{ClFN}_5\text{O}_5\text{Ru}$ ($M + H$) $^+$ 633.9862, found ($M + H$) $^+$ 633.9841.

Complex FL162-1. ^1H NMR (300 MHz, acetone- d_6): δ (ppm) 9.89 (s, 1H), 9.26 (m, 1H), 8.88 (dd, J = 9.3, 2.5 Hz, 1H), 8.21 (dd, J = 2.3, 0.8 Hz, 1H), 8.17 (s, 1H), 7.10-7.02 (m, 2H),

5.44 (m, 2H), 4.95 (m, 2H), 4.71 (m, 1H), 4.49 (m, 1H), 3.84 (m, 1H), 3.16 (m, 1H). HRMS calculated for $C_{24}H_{16}ClFN_5O_6Ru$ ($M + H$)⁺ 625.9811, found ($M + H$)⁺ 625.9795.

Complex FL162-2. 1H NMR (300 MHz, acetone-*d*₆): δ (ppm) 9.84 (s, 1H), 8.74 (dd, *J* = 9.6, 2.4 Hz, 1H), 8.56 (t, *J* = 2.5 Hz, 1H), 8.46 (d, *J* = 8.9 Hz, 1H), 8.23 (d, *J* = 2.6 Hz, 1H), 8.09 (s, 1H), 7.09 (dd, *J* = 8.9, 2.6 Hz, 1H), 5.27 (m, 2H), 4.91 (m, 2H), 4.65 (m, 1H), 4.33 (m, 1H), 3.60 (m, 1H), 3.11 (m, 1H). HRMS calculated for $C_{24}H_{16}ClFN_5O_6Ru$ ($M + H$)⁺ 625.9811, found ($M + H$)⁺ 625.9799.

Complex FL306. 1H NMR (300 MHz, acetone-*d*₆): δ (ppm) 9.85 (s, 1H), 9.59 (dd, *J* = 5.6, 1.1 Hz, 1H), 8.65-8.58 (m, 2H), 8.50 (d, *J* = 7.9 Hz, 1H), 8.41-8.33 (m, 2H), 8.22 (t, *J* = 7.7 Hz, 1H), 7.86-7.82 (m, 2H), 7.63 (m, 1H), 7.42 (d, *J* = 8.2 Hz, 1H), 7.17 (dd, *J* = 8.9, 2.6 Hz, 1H), 7.07 (m, 1H), 6.61 (m, 1H), 5.50 (d, *J* = 8.4 Hz, 1H). HRMS calculated for $C_{30}H_{16}ClFN_6O_4Ru$ ($M + Na$)⁺ 702.9841, found ($M + Na$)⁺ 702.9857.

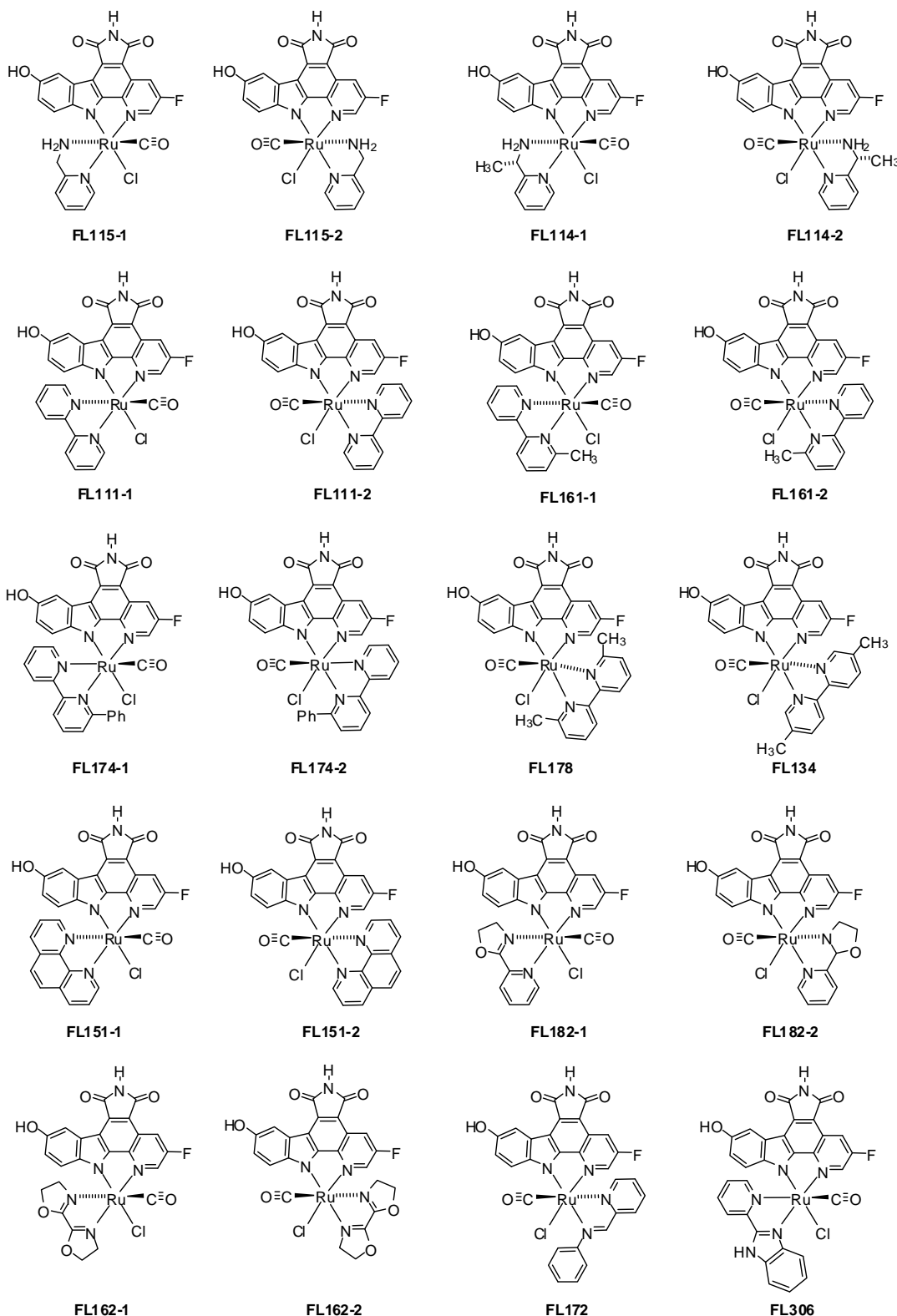


Figure S7. Structures of a library of octahedral complexes with a variety of large and rigid bidentate ligands. All compounds are racemic mixtures, except for **FL114-1** and **FL114-2** which are mixtures of diastereomers.

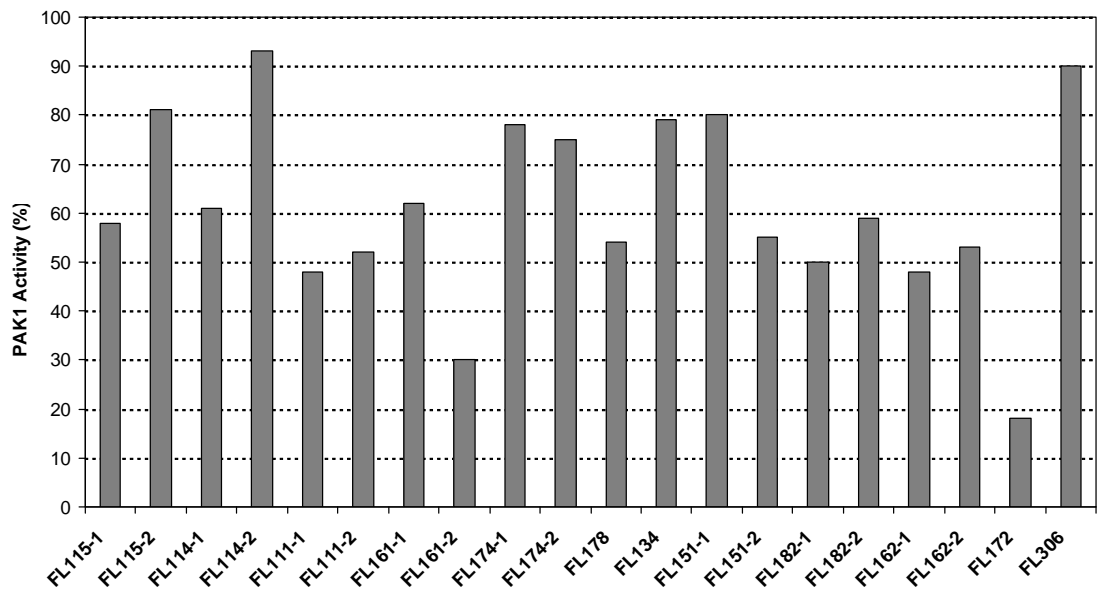


Figure S8. Inhibition of PAK1 by octahedral complexes at a concentration of 1 μM (1 μM ATP).

A.4.) Identification of FL411 from a library of FL172 derivatives

Derivatives of **FL172** were synthesized in analogy to **FL172** by using derivatized 2-(phenylaminomethyl)pyridines (Figure S9a). Kinase inhibition data are shown in Figure S9b,c.

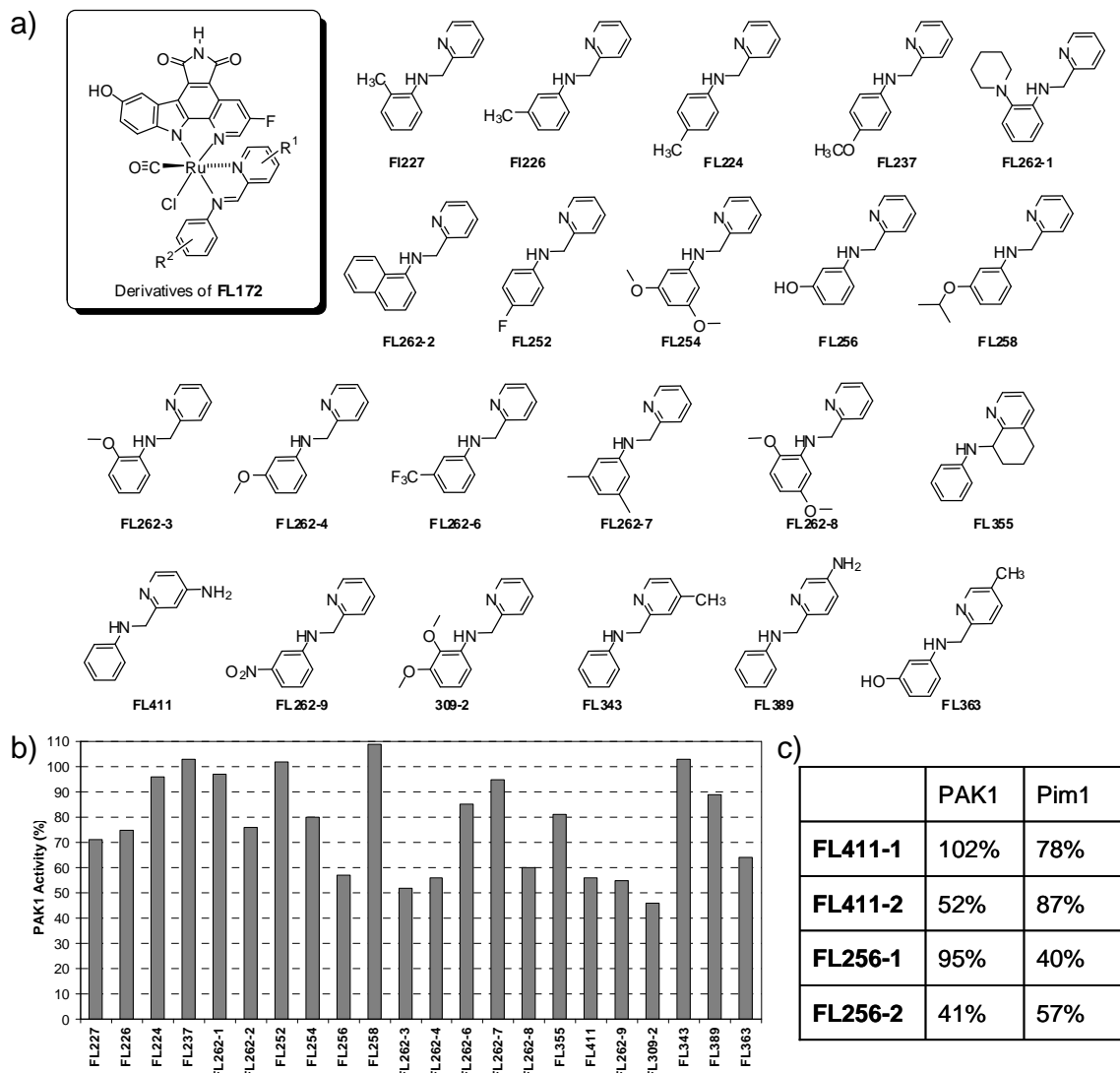


Figure S9. a) Library of **FL172** derivatives. b) Inhibition of PAK1 by racemic derivatives of **FL172** at a concentration of 0.1 μ M (1 μ M ATP). c.) Compounds **FL411** and **FL256** were selected and resolved into their individual enantiomers (**FL411-1**, **FL411-2** and **FL256-1**, **FL256-2**, respectively) by chiral HPLC and measured against PAK1 and Pim1 at a

concentration of 0.1 μ M (1 μ M ATP). **FL411-1** and **FL411-2** were later assigned to Δ -**FL411** and Λ -**FL411**, respectively (see part A.6.)

Complex FL227. ^1H NMR (300 MHz, acetone- d_6): δ (ppm) 9.89 (s, 1H), 9.18 (s, 1H), 8.73 (dd, J = 9.3, 2.4 Hz, 1H), 8.63 (m, 1H), 8.59 (d, J = 8.9 Hz, 1H), 8.42 (m, 1H), 8.31 (d, J = 2.5 Hz, 1H), 8.184 (s, 1H), 8.180 (td, J = 7.8, 1.6 Hz, 1H), 8.05 (d, J = 7.7 Hz, 1H), 7.57-7.35 (m, 5H), 7.12 (dd, J = 8.9, 2.6 Hz, 1H), 2.64 (s, 3H). HRMS calculated for $\text{C}_{31}\text{H}_{19}\text{ClFN}_5\text{O}_4\text{Ru}$ ($\text{M} + \text{Na}$) $^+$ 704.0045, found ($\text{M} + \text{Na}$) $^+$ 704.0043.

Complex FL226. ^1H NMR (300 MHz, acetone- d_6): δ (ppm) 9.88 (s, 1H), 9.21 (s, 1H), 8.69 (dd, J = 9.4, 2.4 Hz, 1H), 8.59 (d, J = 8.9 Hz, 1H), 8.37 (m, 1H), 8.34 (t, J = 2.5 Hz, 1H), 8.31 (d, J = 2.6 Hz, 1H), 8.19 (s, 1H), 8.16 (td, J = 7.7, 1.8 Hz, 1H), 7.95-7.92 (m, 2H), 7.56 (t, J = 7.7 Hz, 1H), 7.49-7.39 (m, 3H), 7.15 (dd, J = 8.9, 2.6 Hz, 1H), 2.52 (s, 3H). HRMS calculated for $\text{C}_{31}\text{H}_{19}\text{ClFN}_5\text{O}_4\text{Ru}$ ($\text{M} + \text{Na}$) $^+$ 704.0045, found ($\text{M} + \text{Na}$) $^+$ 704.0055.

Complex FL224. ^1H NMR (300 MHz, acetone- d_6): δ (ppm) 9.88 (s, 1H), 9.18 (s, 1H), 8.69 (dd, J = 9.4, 2.4 Hz, 1H), 8.59 (d, J = 8.9 Hz, 1H), 8.36 (m, 1H), 8.33-8.31 (m, 2H), 8.20 (s, 1H), 8.15 (td, J = 7.7, 1.8 Hz, 1H), 8.03-8.00 (m, 2H), 7.50-7.40 (m, 4H), 7.15 (dd, J = 8.9, 2.6 Hz, 1H), 2.47 (s, 3H). HRMS calculated for $\text{C}_{31}\text{H}_{20}\text{ClFN}_5\text{O}_4\text{Ru}$ ($\text{M} + \text{H}$) $^+$ 682.0226, found ($\text{M} + \text{H}$) $^+$ 682.0231.

Complex FL237. ^1H NMR (300 MHz, acetone- d_6): δ (ppm) 9.88 (s, 1H), 9.15 (s, 1H), 8.68 (dd, J = 9.4, 2.3 Hz, 1H), 8.59 (d, J = 8.9 Hz, 1H), 8.35-8.30 (m, 3H), 8.19 (s, 1H), 8.16-8.07 (m, 3H), 7.48-7.39 (m, 2H), 7.24-7.19 (m, 2H), 7.15 (dd, J = 8.9, 2.6 Hz, 1H), 3.94 (s, 3H). HRMS calculated for $\text{C}_{31}\text{H}_{19}\text{ClFN}_5\text{O}_6\text{Ru}$ ($\text{M} + \text{Na}$) $^+$ 719.9994, found ($\text{M} + \text{Na}$) $^+$ 719.9999.

Complex FL262-1. HRMS calculated for $\text{C}_{35}\text{H}_{27}\text{ClFN}_6\text{O}_4\text{Ru}$ ($\text{M} + \text{H}$) $^+$ 751.0810, found ($\text{M} + \text{H}$) $^+$ 751.0784.

Complex FL262-2. HRMS calculated for $C_{36}H_{22}FN_6O_4Ru$ ($M - Cl + CH_3CN$)⁺ 723.0730, found ($M - Cl + CH_3CN$)⁺ 723.0787.

Complex FL252. 1H NMR (300 MHz, acetone-*d*₆): δ (ppm) 9.89 (s, 1H), 9.23 (s, 1H), 8.69 (dd, *J* = 9.4, 2.4 Hz, 1H), 8.57 (d, *J* = 8.9 Hz, 1H), 8.38 (m, 1H), 8.36 (t, *J* = 2.5 Hz, 1H), 8.31 (d, *J* = 2.3 Hz, 1H), 8.23-8.14 (m, 4H), 7.51-7.43 (m, 4H), 7.15 (dd, *J* = 8.9, 2.6 Hz, 1H). HRMS calculated for $C_{30}H_{17}ClF_2N_5O_4Ru$ ($M + H$)⁺ 685.9975, found ($M + H$)⁺ 685.9981.

Complex FL254. 1H NMR (300 MHz, acetone-*d*₆): δ (ppm) 9.89 (s, 1H), 9.23 (s, 1H), 8.68 (dd, *J* = 9.4, 2.4 Hz, 1H), 8.59 (d, *J* = 8.9 Hz, 1H), 8.38-8.34 (m, 2H), 8.31 (d, *J* = 2.6 Hz, 1H), 8.21 (s, 1H), 8.16 (td, *J* = 7.6, 1.8 Hz, 1H), 7.50-7.42 (m, 2H), 7.39 (d, *J* = 2.3 Hz, 2H), 7.15 (dd, *J* = 8.9, 2.6 Hz, 1H), 6.67 (t, *J* = 2.2 Hz, 1H), 3.94 (s, 6H). HRMS calculated for $C_{32}H_{22}ClFN_5O_6Ru$ ($M + H$)⁺ 728.0281, found ($M + H$)⁺ 728.0286.

Complex FL256. 1H NMR (300 MHz, acetone-*d*₆): δ (ppm) 9.89 (s, 1H), 9.18 (s, 1H), 9.10 (br, 1H), 8.69 (dd, *J* = 9.4, 2.4 Hz, 1H), 8.59 (d, *J* = 9.2 Hz, 1H), 8.37 (m, 1H), 8.34 (t, *J* = 2.5 Hz, 1H), 8.31 (d, *J* = 2.5 Hz, 1H), 8.21 (s, 1H), 8.15 (td, *J* = 7.7, 1.8 Hz, 1H), 7.62 (t, *J* = 2.1 Hz, 1H), 7.57-7.41 (m, 4H), 7.15 (dd, *J* = 8.9, 2.6 Hz, 1H), 7.04 (m, 1H). HRMS calculated for $C_{30}H_{17}ClFN_5O_5Ru$ ($M + Na$)⁺ 7005.9838, found ($M + Na$)⁺ 705.9897.

Complex FL258. 1H NMR (300 MHz, acetone-*d*₆): δ (ppm) 9.88 (s, 1H), 9.21 (s, 1H), 8.69 (dd, *J* = 9.4, 2.3 Hz, 1H), 8.59 (d, *J* = 8.9 Hz, 1H), 8.37 (m, 1H), 8.34 (t, *J* = 2.5 Hz, 1H), 8.31 (d, *J* = 2.6 Hz, 1H), 8.21 (s, 1H), 8.16 (td, *J* = 7.7, 1.8 Hz, 1H), 7.78 (t, *J* = 2.2 Hz, 1H), 7.66 (m, 1H), 7.55 (t, *J* = 8.0 Hz, 1H), 7.50-7.42 (m, 2H), 7.15 (dd, *J* = 8.9, 2.6 Hz, 1H), 7.11 (m, 1H), 4.81 (m, 1H), 1.41 (m, 6H). HRMS calculated for $C_{33}H_{24}ClFN_5O_5Ru$ ($M + H$)⁺ 726.0488, found ($M + H$)⁺ 726.0508.

Complex FL262-3. ^1H NMR (300 MHz, acetone- d_6): δ (ppm) 9.87 (s, 1H), 9.19 (s, 1H), 8.82 (dd, J = 3.4, 2.4 Hz, 1H), 8.70 (dd, J = 9.2, 2.4 Hz, 1H), 8.58 (d, J = 8.9 Hz, 1H), 8.38 (m, 1H), 8.31 (d, J = 2.6 Hz, 1H), 8.17 (s, 1H), 8.16 (td, J = 7.7, 1.7 Hz, 1H), 8.03 (dd, J = 7.9, 1.6 Hz, 1H), 7.53-7.39 (m, 4H), 7.21 (m, 1H), 7.13 (dd, J = 8.9, 2.6 Hz, 1H), 4.14 (s, 3H). HRMS calculated for $\text{C}_{31}\text{H}_{19}\text{ClFN}_5\text{O}_6\text{Ru}$ ($\text{M} + \text{Na}$) $^+$ 719.9994, found ($\text{M} + \text{Na}$) $^+$ 720.0002. And the amino-complex is also isolated in this reaction: ^1H NMR (300 MHz, acetone- d_6): δ (ppm) 9.87 (s, 1H), 9.24 (dd, J = 3.9, 2.4 Hz, 1H), 8.81 (dd, J = 9.2, 2.4 Hz, 1H), 8.58 (d, J = 8.9 Hz, 1H), 8.27 (d, J = 2.5 Hz, 1H), 8.16 (m, 1H), 8.11 (s, 1H), 7.89 (td, J = 7.3, 2.0 Hz, 1H), 7.79-7.72 (m, 2H), 7.32-7.23 (m, 2H), 7.14-7.03 (m, 4H), 5.81 (dd, J = 14.1, 10.9 Hz, 1H), 4.54 (dd, J = 14.4, 3.9 Hz, 1H), 4.13 (s, 3H).

Complex FL262-4. HRMS calculated for $\text{C}_{31}\text{H}_{19}\text{ClFN}_5\text{O}_6\text{Ru}$ ($\text{M} + \text{Na}$) $^+$ 719.9994, found ($\text{M} + \text{Na}$) $^+$ 719.9998.

Complex FL262-6. HRMS calculated for $\text{C}_{31}\text{H}_{16}\text{Cl}_2\text{F}_4\text{N}_5\text{O}_4\text{Ru}$ ($\text{M} + \text{Cl}$) $^-$ 769.9559, found ($\text{M} + \text{Cl}$) $^-$ 769.9484.

Complex FL262-7. HRMS calculated for $\text{C}_{34}\text{H}_{24}\text{FN}_6\text{O}_4\text{Ru}$ ($\text{M} - \text{Cl} + \text{CH}_3\text{CN}$) $^+$ 701.0887, found ($\text{M} - \text{Cl} + \text{CH}_3\text{CN}$) $^+$ 701.0856.

Complex FL262-8. HRMS calculated for $\text{C}_{32}\text{H}_{22}\text{ClFN}_5\text{O}_6\text{Ru}$ ($\text{M} + \text{H}$) $^+$ 728.0281, found ($\text{M} + \text{H}$) $^+$ 728.0287.

Complex FL355. ^1H NMR (300 MHz, acetone- d_6): δ (ppm) 9.86 (s, 1H), 8.69 (dd, J = 9.4, 2.3 Hz, 1H), 8.58-8.55 (m, 2H), 8.29 (d, d , J = 2.6 Hz, 1H), 8.17 (s, 1H), 7.97-7.34 (m, 8H), 7.12 (dd, J = 8.9, 2.6 Hz, 1H), 3.39-2.99 (m, 4H), 2.18 (m, 1H), 1.90 (m, 1H). HRMS calculated for $\text{C}_{33}\text{H}_{22}\text{ClFN}_5\text{O}_4\text{Ru}$ ($\text{M} + \text{H}$) $^+$ 708.0382, found ($\text{M} + \text{H}$) $^+$ 708.0386.

Complex FL262-9. ^1H NMR (300 MHz, acetone- d_6): δ (ppm) 9.90 (s, 1H), 9.42 (s, 1H), 9.00 (t, J = 2.1 Hz, 1H), 8.71-8.65 (m, 2H), 8.58 (d, J = 8.9 Hz, 1H), 8.48-8.45 (m, 3H), 8.31 (d, J = 2.6 Hz, 1H), 8.21 (s, 1H), 8.21 (td, J = 6.9, 2.5 Hz, 1H), 8.03 (t, J = 8.2 Hz, 1H), 7.54-7.48 (m, 2H), 7.16 (dd, J = 8.9, 2.6 Hz, 1H). HRMS calculated for $\text{C}_{30}\text{H}_{17}\text{ClFN}_6\text{O}_6\text{Ru}$ ($M + \text{H}$) $^+$ 712.9920, found ($M + \text{H}$) $^+$ 712.9949.

Complex FL309-2. HRMS calculated for $\text{C}_{32}\text{H}_{22}\text{ClFN}_5\text{O}_6\text{Ru}$ ($M + \text{H}$) $^+$ 728.0281, found ($M + \text{H}$) $^+$ 728.0291.

Complex FL343. ^1H NMR (300 MHz, acetone- d_6): δ (ppm) 9.88 (s, 1H), 9.13 (s, 1H), 8.69 (dd, J = 9.4, 2.4 Hz, 1H), 8.58 (d, J = 8.9 Hz, 1H), 8.34 (t, J = 2.5 Hz, 1H), 8.31 (d, J = 2.5 Hz, 1H), 8.20 (s, 1H), 8.18 (m, 1H), 8.13-8.09 (m, 2H), 7.72-7.65 (m, 2H), 7.58 (m, 1H), 7.31-7.24 (m, 2H), 7.15 (dd, J = 8.9, 2.6 Hz, 1H), 2.47 (s, 3H). HRMS calculated for $\text{C}_{31}\text{H}_{19}\text{ClFN}_5\text{O}_4\text{Ru}$ ($M + \text{Na}$) $^+$ 704.0045, found ($M + \text{Na}$) $^+$ 704.0047.

Complex FL389. ^1H NMR (300 MHz, acetone- d_6): δ (ppm) 9.87 (s, 1H), 8.83 (s, 1H), 8.70 (dd, J = 9.4, 2.4 Hz, 1H), 8.59 (d, J = 8.9 Hz, 1H), 8.31 (t, J = 2.5 Hz, 1H), 8.27 (d, J = 2.5 Hz, 1H), 8.19 (s, 1H), 8.07-8.02 (m, 2H), 7.98 (d, J = 8.6 Hz, 1H), 7.64-7.58 (m, 2H), 7.49 (m, 1H), 7.19-7.11 (m, 2H), 7.05 (d, J = 2.6 Hz, 1H), 6.06 (s, 2H). HRMS calculated for $\text{C}_{30}\text{H}_{18}\text{ClFN}_6\text{O}_4\text{Ru}$ ($M + \text{Na}$) $^+$ 704.9998, found ($M + \text{Na}$) $^+$ 704.9999.

Complex FL363. ^1H NMR (300 MHz, acetone- d_6): δ (ppm) 9.88 (s, 1H), 9.12 (s, 1H), 9.06 (s, 1H), 8.69 (dd, J = 9.5, 2.4 Hz, 1H), 8.59 (d, J = 8.9 Hz, 1H), 8.33 (t, J = 2.5 Hz, 1H), 8.31 (d, J = 2.6 Hz, 1H), 8.26 (d, J = 8.0 Hz, 1H), 8.20 (s, 1H), 7.96 (m, 1H), 7.59 (m, 1H), 7.53 (m, 1H), 7.47 (t, J = 7.9 Hz, 1H), 7.39 (m, 1H), 7.15 (dd, J = 8.9, 2.6 Hz, 1H), 7.02 (m, 1H), 2.01 (s, 3H). HRMS calculated for $\text{C}_{31}\text{H}_{20}\text{ClFN}_5\text{O}_5\text{Ru}$ ($M + \text{H}$) $^+$ 698.0175, found ($M + \text{H}$) $^+$ 698.0178.

A.5.) Crystallographic data of FL389 for the determination of the relative configurations of FL172 and FL411

Crystal structure of FL389. This crystal structure verifies the relative configuration of the related complexes **FL172** and **FL411**. **FL389** was synthesized by analogy to **FL172** and **FL411** by reacting precursor **3** first with CO and then 2-(phenylaminomethyl)-5-aminopyridine. Crystals of **FL389** were grown in deuterated acetone overnight.

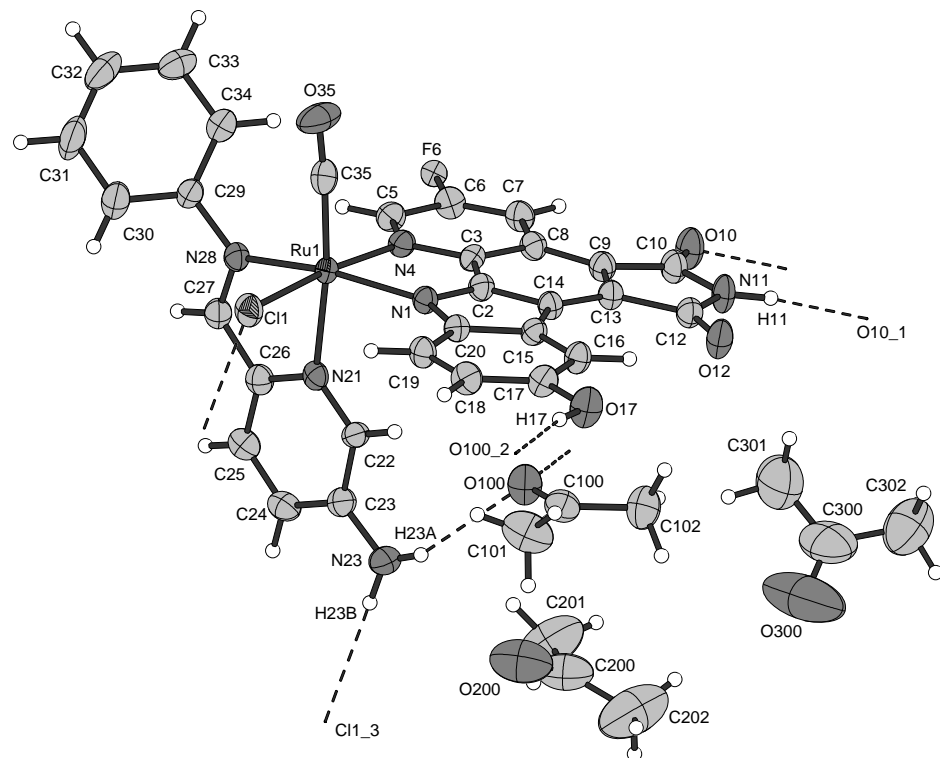


Figure S10. ORTEP drawing of compound **FL389** with 50% probability thermal ellipsoid.

Table S1. Crystal data and structure refinement for **FL389**.

Crystal data

Identification code	FL389
Habitus, colour	prism, red
Crystal size	0.27 x 0.09 x 0.02 mm ³
Crystal system	Triclinic
Space group	P $\bar{1}$
Unit cell dimensions	$a = 7.6625(3)$ Å $\alpha = 101.764(3)^\circ$ $b = 15.8593(6)$ Å $\beta = 92.604(3)^\circ$ $c = 15.9895(5)$ Å $\gamma = 96.270(3)^\circ$ $1886.30(12)$ Å ³
Volume	$1886.30(12)$ Å ³
Cell determination	18229 peaks with Theta 4.5 to 25°.
Empirical formula	C ₃₉ H ₃₆ Cl F N ₆ O ₇ Ru
Formula weight	856.26
Density (calculated)	1.508 Mg/m ³
Absorption coefficient	0.550 mm ⁻¹
F(000)	876

Data collection:

Diffractometer type	IPDS 2T
Wavelength	0.71073 Å
Temperature	193(2) K
Theta range for data collection	4.64 to 25.00°.
Index ranges	-8≤h≤9, -18≤k≤18, -18≤l≤18
Data collection software	STOE WinXpose (X-Area)
Cell refinement software	STOE WinCell (X-Area)
Data reduction software	STOE WinIntegrate (X-Area)

Solution and refinement:

Reflections collected	16388
Independent reflections	6276 [R(int) = 0.0611]
Completeness to theta = 25.00°	94.7 %
Observed reflections	5215[I>2sigma(I)]
Reflections used for refinement	6276
Absorption correction	Semi-empirical from equivalents
Max. and min. transmission	0.9761 and 0.9054
Largest diff. peak and hole	0.615 and -0.595 e.Å ⁻³
Solution	Direct methods
Refinement	Full-matrix least-squares on F ²
Treatment of hydrogen atoms	Calculated positions, riding model
Programs used	SIR92 SHELXL-97 Diamond 3.1, STOE IPDS2 software
Data / restraints / parameters	6276 / 0 / 503
Goodness-of-fit on F ²	1.066
R index (all data)	wR2 = 0.1015
R index conventional [I>2sigma(I)]	R1 = 0.0454

SIR92: Atomare, A.; Cascarano, G.; Giacovazzo, C.; Guagliardi, A.; Burla, M. C.; Polidori, G.; Camalli, M. *J. Appl. Cryst.* **1994**, *27*, 435.

SHELXL-97: Program for the Refinement of Crystal Structures, G. M. Sheldrick (1997), University of Göttingen, Germany.

Table S2. Atomic coordinates and equivalent isotropic displacement parameters (\AA^2) for **FL389**. U(eq) is defined as one third of the trace of the orthogonalized U_{ij} tensor.

	x	y	z	U(eq)	Occupancy
C2	0.9858(5)	0.8349(2)	0.1618(2)	0.0266(7)	1
C3	0.8261(5)	0.8562(2)	0.1302(2)	0.0261(7)	1
C5	0.6536(5)	0.9653(3)	0.1209(2)	0.0302(8)	1
C6	0.5258(5)	0.9026(3)	0.0738(2)	0.0306(8)	1
C7	0.5400(5)	0.8171(3)	0.0544(2)	0.0299(8)	1
C8	0.6975(5)	0.7907(2)	0.0842(2)	0.0269(8)	1
C9	0.7386(5)	0.7042(2)	0.0738(2)	0.0284(8)	1
C10	0.6278(5)	0.6231(3)	0.0361(2)	0.0331(8)	1
C12	0.8913(5)	0.5878(2)	0.0853(2)	0.0301(8)	1
C13	0.8974(5)	0.6840(2)	0.1047(2)	0.0274(8)	1
C14	1.0284(5)	0.7487(2)	0.1489(2)	0.0251(7)	1
C15	1.2021(5)	0.7575(2)	0.1900(2)	0.0250(7)	1
C16	1.3197(5)	0.6976(2)	0.1999(2)	0.0291(8)	1
C17	1.4780(5)	0.7285(3)	0.2461(2)	0.0318(8)	1
C18	1.5214(5)	0.8175(3)	0.2817(2)	0.0336(9)	1
C19	1.4090(5)	0.8778(3)	0.2718(2)	0.0293(8)	1
C20	1.2472(5)	0.8476(2)	0.2250(2)	0.0258(7)	1
C22	0.9090(5)	0.9434(2)	0.3781(2)	0.0273(8)	1
C23	0.8225(5)	0.9435(3)	0.4540(2)	0.0307(8)	1
C24	0.7244(5)	1.0111(3)	0.4832(2)	0.0338(9)	1
C25	0.7137(5)	1.0742(3)	0.4364(2)	0.0335(8)	1
C26	0.8023(5)	1.0716(3)	0.3624(2)	0.0297(8)	1
C27	0.8084(5)	1.1375(2)	0.3121(2)	0.0299(8)	1
C29	0.9124(5)	1.1998(2)	0.2009(2)	0.0299(8)	1
C30	0.9526(6)	1.2837(3)	0.2455(3)	0.0444(10)	1
C31	0.9619(8)	1.3500(3)	0.2001(4)	0.0580(13)	1
C32	0.9351(7)	1.3328(3)	0.1132(4)	0.0544(13)	1
C33	0.8963(6)	1.2492(3)	0.0691(3)	0.0423(10)	1
C34	0.8854(5)	1.1816(3)	0.1125(3)	0.0344(9)	1
C35	1.1277(5)	1.0440(3)	0.1246(3)	0.0364(9)	1
C100	1.0162(5)	0.6820(3)	0.3567(3)	0.0391(9)	1
C101	1.1883(7)	0.7120(5)	0.4063(3)	0.0656(15)	1
C102	0.9732(8)	0.5880(3)	0.3180(4)	0.0597(13)	1
C200	0.7674(8)	0.6397(5)	0.5249(4)	0.0740(18)	1
C201	0.6022(9)	0.6670(6)	0.4963(6)	0.107(3)	1
C202	0.7641(13)	0.5499(7)	0.5341(7)	0.131(4)	1
C300	0.4902(10)	0.3734(6)	0.2514(5)	0.093(2)	1
C301	0.4610(14)	0.4464(6)	0.2101(6)	0.117(3)	1
C302	0.4465(10)	0.2855(5)	0.1952(6)	0.097(2)	1
N1	1.1115(4)	0.89448(19)	0.20618(18)	0.0250(6)	1
N4	0.8050(4)	0.9425(2)	0.14865(19)	0.0268(6)	1
N11	0.7273(4)	0.5566(2)	0.0439(2)	0.0354(7)	1
N21	0.8985(4)	1.0059(2)	0.33386(18)	0.0260(6)	1
N23	0.8349(5)	0.8776(2)	0.4957(2)	0.0382(8)	1
N28	0.8996(4)	1.1292(2)	0.24563(19)	0.0280(7)	1
O10	0.4769(4)	0.61258(18)	0.0048(2)	0.0412(7)	1
O12	1.0021(4)	0.54371(18)	0.10187(19)	0.0402(7)	1
O17	1.5908(4)	0.66924(19)	0.2565(2)	0.0425(7)	1
O35	1.1887(5)	1.0651(2)	0.0663(2)	0.0584(10)	1
O100	0.9119(4)	0.7331(2)	0.3491(2)	0.0466(7)	1
O200	0.9018(6)	0.6908(4)	0.5387(3)	0.0906(15)	1
O300	0.5472(12)	0.3858(7)	0.3235(4)	0.175(4)	1
F6	0.3789(3)	0.93192(16)	0.04606(16)	0.0457(6)	1
C11	1.28290(12)	1.09337(6)	0.30739(6)	0.0342(2)	1
Ru1	1.02562(4)	1.01860(2)	0.21998(2)	0.02367(10)	1

Table S3. Bond lengths [Å] and angles [°] for **FL389**.

C2-N1	1.339(5)	C29-N28	1.443(4)
C2-C3	1.403(5)	C30-C31	1.391(6)
C2-C14	1.417(5)	C30-H30	0.9500
C3-N4	1.370(5)	C31-C32	1.362(8)
C3-C8	1.412(5)	C31-H31	0.9500
C5-N4	1.336(5)	C32-C33	1.362(7)
C5-C6	1.388(5)	C32-H32	0.9500
C5-H5	0.9500	C33-C34	1.388(5)
C6-C7	1.346(6)	C33-H33	0.9500
C6-F6	1.354(4)	C34-H34	0.9500
C7-C8	1.413(5)	C35-O35	1.155(5)
C7-H7	0.9500	C35-Ru1	1.841(4)
C8-C9	1.420(5)	C100-O100	1.218(5)
C9-C13	1.386(5)	C100-C101	1.486(7)
C9-C10	1.462(5)	C100-C102	1.487(7)
C10-O10	1.219(5)	C101-H10A	0.9800
C10-N11	1.389(5)	C101-H10B	0.9800
C12-O12	1.211(5)	C101-H10C	0.9800
C12-N11	1.384(5)	C102-H10D	0.9800
C12-C13	1.489(5)	C102-H10E	0.9800
C13-C14	1.405(5)	C102-H10F	0.9800
C14-C15	1.437(5)	C200-O200	1.220(8)
C15-C16	1.406(5)	C200-C202	1.459(11)
C15-C20	1.422(5)	C200-C201	1.465(9)
C16-C17	1.378(5)	C201-H20A	0.9800
C16-H16	0.9500	C201-H20B	0.9800
C17-O17	1.374(5)	C201-H20C	0.9800
C17-C18	1.407(6)	C202-H20D	0.9800
C18-C19	1.382(6)	C202-H20E	0.9800
C18-H18	0.9500	C202-H20F	0.9800
C19-C20	1.402(5)	C300-O300	1.184(9)
C19-H19	0.9500	C300-C301	1.476(12)
C20-N1	1.399(5)	C300-C302	1.492(11)
C22-N21	1.337(4)	C301-H30A	0.9800
C22-C23	1.408(5)	C301-H30B	0.9800
C22-H22	0.9500	C301-H30C	0.9800
C23-N23	1.358(5)	C302-H30D	0.9800
C23-C24	1.391(6)	C302-H30E	0.9800
C24-C25	1.375(5)	C302-H30F	0.9800
C24-H24	0.9500	N1-Ru1	2.116(3)
C25-C26	1.386(5)	N4-Ru1	2.105(3)
C25-H25	0.9500	N11-H11	0.8800
C26-N21	1.357(5)	N21-Ru1	2.138(3)
C26-C27	1.442(5)	N23-H23A	0.8020
C27-N28	1.291(5)	N23-H23B	0.8879
C27-H27	0.9500	N28-Ru1	2.071(3)
C29-C30	1.371(6)	O17-H17	0.8400
C29-C34	1.385(5)	Cl1-Ru1	2.4102(9)
N1-C2-C3	122.7(3)	C7-C6-C5	124.6(3)
N1-C2-C14	114.2(3)	F6-C6-C5	116.0(3)
C3-C2-C14	123.0(3)	C6-C7-C8	116.7(3)
N4-C3-C2	115.8(3)	C6-C7-H7	121.6
N4-C3-C8	123.8(3)	C8-C7-H7	121.6
C2-C3-C8	120.4(3)	C3-C8-C7	117.2(3)
N4-C5-C6	120.1(4)	C3-C8-C9	116.3(3)
N4-C5-H5	120.0	C7-C8-C9	126.5(3)
C6-C5-H5	120.0	C13-C9-C8	122.7(3)
C7-C6-F6	119.4(3)	C13-C9-C10	108.3(3)

C8-C9-C10	128.9(3)	C32-C33-C34	120.2(4)
O10-C10-N11	124.9(4)	C32-C33-H33	119.9
O10-C10-C9	128.8(4)	C34-C33-H33	119.9
N11-C10-C9	106.3(3)	C29-C34-C33	119.5(4)
O12-C12-N11	125.5(4)	C29-C34-H34	120.2
O12-C12-C13	129.0(3)	C33-C34-H34	120.2
N11-C12-C13	105.5(3)	O35-C35-Ru1	175.7(4)
C9-C13-C14	121.7(3)	O100-C100-C101	120.7(5)
C9-C13-C12	107.8(3)	O100-C100-C102	120.9(4)
C14-C13-C12	130.5(3)	C101-C100-C102	118.5(5)
C13-C14-C2	115.8(3)	C100-C101-H10A	109.5
C13-C14-C15	140.2(3)	C100-C101-H10B	109.5
C2-C14-C15	104.0(3)	H10A-C101-H10B	109.5
C16-C15-C20	120.9(3)	C100-C101-H10C	109.5
C16-C15-C14	133.1(3)	H10A-C101-H10C	109.5
C20-C15-C14	106.1(3)	H10B-C101-H10C	109.5
C17-C16-C15	118.0(4)	C100-C102-H10D	109.5
C17-C16-H16	121.0	C100-C102-H10E	109.5
C15-C16-H16	121.0	H10D-C102-H10E	109.5
O17-C17-C16	117.6(4)	C100-C102-H10F	109.5
O17-C17-C18	121.4(3)	H10D-C102-H10F	109.5
C16-C17-C18	121.0(4)	H10E-C102-H10F	109.5
C19-C18-C17	122.0(3)	O200-C200-C202	122.3(7)
C19-C18-H18	119.0	O200-C200-C201	120.3(7)
C17-C18-H18	119.0	C202-C200-C201	117.4(7)
C18-C19-C20	117.8(4)	C200-C201-H20A	109.5
C18-C19-H19	121.1	C200-C201-H20B	109.5
C20-C19-H19	121.1	H20A-C201-H20B	109.5
N1-C20-C19	129.1(3)	C200-C201-H20C	109.5
N1-C20-C15	110.7(3)	H20A-C201-H20C	109.5
C19-C20-C15	120.3(3)	H20B-C201-H20C	109.5
N21-C22-C23	121.9(4)	C200-C202-H20D	109.5
N21-C22-H22	119.1	C200-C202-H20E	109.5
C23-C22-H22	119.1	H20D-C202-H20E	109.5
N23-C23-C24	122.0(4)	C200-C202-H20F	109.5
N23-C23-C22	119.5(4)	H20D-C202-H20F	109.5
C24-C23-C22	118.5(3)	H20E-C202-H20F	109.5
C25-C24-C23	118.8(3)	O300-C300-C301	121.1(10)
C25-C24-H24	120.6	O300-C300-C302	123.8(10)
C23-C24-H24	120.6	C301-C300-C302	115.1(7)
C24-C25-C26	120.5(4)	C300-C301-H30A	109.5
C24-C25-H25	119.7	C300-C301-H30B	109.5
C26-C25-H25	119.7	H30A-C301-H30B	109.5
N21-C26-C25	120.8(3)	C300-C301-H30C	109.5
N21-C26-C27	114.5(3)	H30A-C301-H30C	109.5
C25-C26-C27	124.6(4)	H30B-C301-H30C	109.5
N28-C27-C26	119.1(4)	C300-C302-H30D	109.5
N28-C27-H27	120.5	C300-C302-H30E	109.5
C26-C27-H27	120.5	H30D-C302-H30E	109.5
C30-C29-C34	120.5(4)	C300-C302-H30F	109.5
C30-C29-N28	120.2(3)	H30D-C302-H30F	109.5
C34-C29-N28	119.3(3)	H30E-C302-H30F	109.5
C29-C30-C31	118.5(4)	C2-N1-C20	105.1(3)
C29-C30-H30	120.7	C2-N1-Ru1	109.1(2)
C31-C30-H30	120.7	C20-N1-Ru1	145.8(2)
C32-C31-C30	121.4(5)	C5-N4-C3	117.6(3)
C32-C31-H31	119.3	C5-N4-Ru1	130.5(3)
C30-C31-H31	119.3	C3-N4-Ru1	111.9(2)
C31-C32-C33	119.8(4)	C12-N11-C10	112.1(3)
C31-C32-H32	120.1	C12-N11-H11	124.0
C33-C32-H32	120.1	C10-N11-H11	124.0

C22-N21-C26	119.5(3)	C35-Ru1-N1	95.05(15)
C22-N21-Ru1	127.2(3)	N28-Ru1-N1	168.31(11)
C26-N21-Ru1	113.3(2)	N4-Ru1-N1	80.42(11)
C23-N23-H23A	119.1	C35-Ru1-N21	172.58(15)
C23-N23-H23B	116.0	N28-Ru1-N21	77.43(12)
H23A-N23-H23B	124.9	N4-Ru1-N21	88.25(11)
C27-N28-C29	117.1(3)	N1-Ru1-N21	92.34(11)
C27-N28-Ru1	115.7(2)	C35-Ru1-Cl1	89.47(13)
C29-N28-Ru1	127.1(2)	N28-Ru1-Cl1	90.89(9)
C17-O17-H17	109.5	N4-Ru1-Cl1	174.35(8)
C35-Ru1-N28	95.29(15)	N1-Ru1-Cl1	94.65(8)
C35-Ru1-N4	93.70(15)	N21-Ru1-Cl1	89.21(8)
N28-Ru1-N4	93.47(12)		

Table S4. Anisotropic displacement parameters (\AA^2) for **FL389**.

The anisotropic displacement factor exponent takes the form: $-2\pi^2[\ h^2a^*{}^2U^{11} + \dots + 2 h k a^* b^* U^{12}]$

	U ¹¹	U ²²	U ³³	U ²³	U ¹³	U ¹²
C2	0.0272(19)	0.0242(19)	0.0271(18)	0.0050(15)	-0.0007(14)	-0.0006(15)
C3	0.0296(19)	0.0217(18)	0.0271(18)	0.0071(15)	0.0013(14)	0.0007(15)
C5	0.031(2)	0.030(2)	0.0314(19)	0.0076(16)	0.0012(15)	0.0068(16)
C6	0.0236(18)	0.034(2)	0.035(2)	0.0059(17)	-0.0018(15)	0.0076(15)
C7	0.0251(18)	0.031(2)	0.0309(19)	0.0040(16)	-0.0038(14)	0.0005(15)
C8	0.0250(18)	0.0262(19)	0.0276(18)	0.0033(15)	-0.0001(14)	0.0003(15)
C9	0.0270(19)	0.0263(19)	0.0300(19)	0.0037(15)	-0.0025(14)	0.0011(15)
C10	0.034(2)	0.026(2)	0.036(2)	0.0023(16)	-0.0050(16)	-0.0017(16)
C12	0.033(2)	0.0245(19)	0.0311(19)	0.0045(16)	-0.0026(15)	0.0012(16)
C13	0.0283(19)	0.0226(19)	0.0297(18)	0.0032(15)	0.0001(14)	0.0013(15)
C14	0.0250(18)	0.0226(18)	0.0261(17)	0.0025(14)	-0.0010(14)	0.0021(14)
C15	0.0238(18)	0.0236(18)	0.0270(18)	0.0060(15)	-0.0013(14)	-0.0002(14)
C16	0.0250(18)	0.0250(19)	0.036(2)	0.0049(16)	-0.0020(15)	0.0005(15)
C17	0.0264(19)	0.031(2)	0.038(2)	0.0085(17)	-0.0019(15)	0.0021(16)
C18	0.0244(19)	0.036(2)	0.037(2)	0.0056(17)	-0.0060(15)	-0.0046(16)
C19	0.0255(18)	0.027(2)	0.0322(19)	0.0026(16)	-0.0034(14)	-0.0022(15)
C20	0.0275(18)	0.0236(18)	0.0254(17)	0.0043(15)	0.0007(14)	0.0011(15)
C22	0.0304(19)	0.0266(19)	0.0244(18)	0.0080(15)	-0.0019(14)	-0.0023(15)
C23	0.0290(19)	0.030(2)	0.0297(19)	0.0064(16)	-0.0042(15)	-0.0079(16)
C24	0.028(2)	0.042(2)	0.0281(19)	0.0048(17)	0.0034(15)	-0.0027(17)
C25	0.0283(19)	0.039(2)	0.0313(19)	0.0038(17)	0.0012(15)	0.0034(17)
C26	0.0273(19)	0.029(2)	0.0312(19)	0.0036(16)	-0.0025(15)	0.0024(15)
C27	0.0310(19)	0.0260(19)	0.0314(19)	0.0042(16)	-0.0009(15)	0.0032(15)
C29	0.034(2)	0.0237(19)	0.0326(19)	0.0075(16)	0.0033(15)	0.0035(15)
C30	0.055(3)	0.027(2)	0.050(3)	0.0053(19)	0.006(2)	0.0029(19)
C31	0.079(4)	0.022(2)	0.074(4)	0.010(2)	0.016(3)	0.006(2)
C32	0.065(3)	0.036(3)	0.072(3)	0.029(3)	0.013(3)	0.012(2)
C33	0.044(2)	0.046(3)	0.045(2)	0.024(2)	0.0071(19)	0.013(2)
C34	0.032(2)	0.030(2)	0.041(2)	0.0100(18)	0.0012(16)	0.0035(16)
C35	0.041(2)	0.025(2)	0.043(2)	0.0027(18)	0.0045(18)	0.0093(17)
C100	0.037(2)	0.045(3)	0.036(2)	0.0077(19)	0.0042(17)	0.007(2)
C101	0.042(3)	0.098(5)	0.054(3)	0.011(3)	-0.002(2)	0.009(3)
C102	0.076(4)	0.039(3)	0.065(3)	0.007(2)	0.006(3)	0.016(3)
C200	0.060(4)	0.112(5)	0.057(3)	0.034(4)	0.010(3)	0.009(4)
C201	0.059(4)	0.126(7)	0.156(8)	0.085(6)	0.003(4)	0.004(4)
C202	0.129(8)	0.141(9)	0.163(9)	0.094(8)	0.060(7)	0.056(7)
C300	0.089(5)	0.123(7)	0.068(4)	0.026(4)	0.030(4)	-0.007(4)
C301	0.153(8)	0.084(6)	0.101(6)	0.007(5)	0.022(6)	-0.023(5)
C302	0.087(5)	0.080(5)	0.130(7)	0.033(5)	0.028(5)	0.014(4)
N1	0.0248(15)	0.0224(16)	0.0260(15)	0.0034(12)	0.0007(11)	-0.0010(12)
N4	0.0295(16)	0.0249(16)	0.0271(15)	0.0066(13)	0.0030(12)	0.0057(13)
N11	0.0328(18)	0.0197(16)	0.0480(19)	-0.0005(14)	-0.0072(14)	-0.0034(13)
N21	0.0224(15)	0.0246(16)	0.0276(15)	0.0017(13)	-0.0014(12)	-0.0035(12)
N23	0.047(2)	0.0354(19)	0.0321(17)	0.0107(15)	0.0040(14)	-0.0031(15)
N28	0.0310(16)	0.0229(16)	0.0278(16)	0.0032(13)	-0.0020(13)	-0.0006(13)
O10	0.0329(16)	0.0285(15)	0.0564(18)	0.0018(13)	-0.0125(13)	-0.0027(12)
O12	0.0411(16)	0.0235(14)	0.0526(17)	0.0039(13)	-0.0132(13)	0.0034(12)
O17	0.0307(15)	0.0361(16)	0.0591(19)	0.0086(14)	-0.0123(13)	0.0066(12)
O35	0.079(2)	0.059(2)	0.056(2)	0.0341(18)	0.0395(18)	0.0349(19)
O100	0.0412(17)	0.0410(18)	0.0551(19)	0.0056(15)	-0.0040(14)	0.0063(14)
O200	0.062(3)	0.142(5)	0.071(3)	0.035(3)	0.004(2)	0.004(3)
O300	0.185(8)	0.263(11)	0.072(4)	0.034(5)	0.015(4)	-0.003(7)
F6	0.0336(13)	0.0417(14)	0.0595(15)	0.0037(12)	-0.0123(11)	0.0142(11)
C11	0.0325(5)	0.0293(5)	0.0362(5)	0.0018(4)	-0.0014(4)	-0.0062(4)
Ru1	0.02657(16)	0.01878(15)	0.02449(15)	0.00348(11)	0.00129(10)	-0.00018(10)

Table S5. Hydrogen coordinates and isotropic displacement parameters (\AA^2) for **FL389**.

	x	y	z	U(eq)	Occupancy
H5	0.6332	1.0245	0.1333	0.036	1
H7	0.4486	0.7765	0.0224	0.036	1
H16	1.2909	0.6376	0.1754	0.035	1
H18	1.6313	0.8368	0.3134	0.040	1
H19	1.4403	0.9377	0.2960	0.035	1
H22	0.9767	0.8977	0.3578	0.033	1
H24	0.6659	1.0135	0.5346	0.041	1
H25	0.6450	1.1201	0.4548	0.040	1
H27	0.7462	1.1864	0.3276	0.036	1
H30	0.9737	1.2964	0.3060	0.053	1
H31	0.9875	1.4085	0.2304	0.070	1
H32	0.9435	1.3790	0.0834	0.065	1
H33	0.8766	1.2372	0.0086	0.051	1
H34	0.8595	1.1233	0.0818	0.041	1
H10A	1.2143	0.7750	0.4131	0.098	1
H10B	1.2810	0.6835	0.3756	0.098	1
H10C	1.1830	0.6973	0.4628	0.098	1
H10D	0.9957	0.5540	0.3612	0.090	1
H10E	1.0467	0.5721	0.2700	0.090	1
H10F	0.8488	0.5759	0.2973	0.090	1
H20A	0.6276	0.7202	0.4745	0.160	1
H20B	0.5276	0.6780	0.5446	0.160	1
H20C	0.5410	0.6211	0.4507	0.160	1
H20D	0.7276	0.5109	0.4788	0.196	1
H20E	0.6806	0.5387	0.5763	0.196	1
H20F	0.8818	0.5399	0.5534	0.196	1
H30A	0.4923	0.5013	0.2516	0.175	1
H30B	0.3368	0.4412	0.1900	0.175	1
H30C	0.5345	0.4451	0.1614	0.175	1
H30D	0.4396	0.2416	0.2304	0.145	1
H30E	0.5382	0.2747	0.1549	0.145	1
H30F	0.3330	0.2824	0.1632	0.145	1
H11	0.6904	0.5012	0.0249	0.042	1
H23A	0.8804	0.8364	0.4734	0.046	1
H23B	0.7923	0.8846	0.5470	0.046	1
H17	1.6827	0.6951	0.2852	0.064	1

Table S6. Torsion angles [°] for **FL389**.

N1-C2-C3-N4	-0.9(5)	C24-C25-C26-N21	1.2(6)
C14-C2-C3-N4	179.7(3)	C24-C25-C26-C27	-175.8(3)
N1-C2-C3-C8	-179.7(3)	N21-C26-C27-N28	0.7(5)
C14-C2-C3-C8	0.9(5)	C25-C26-C27-N28	178.0(4)
N4-C5-C6-C7	1.6(6)	C34-C29-C30-C31	1.3(7)
N4-C5-C6-F6	-178.0(3)	N28-C29-C30-C31	-179.3(4)
F6-C6-C7-C8	179.1(3)	C29-C30-C31-C32	-1.2(8)
C5-C6-C7-C8	-0.5(6)	C30-C31-C32-C33	0.8(8)
N4-C3-C8-C7	1.2(5)	C31-C32-C33-C34	-0.5(7)
C2-C3-C8-C7	179.9(3)	C30-C29-C34-C33	-1.1(6)
N4-C3-C8-C9	-177.6(3)	N28-C29-C34-C33	179.6(4)
C2-C3-C8-C9	1.1(5)	C32-C33-C34-C29	0.7(6)
C6-C7-C8-C3	-0.8(5)	C3-C2-N1-C20	-179.6(3)
C6-C7-C8-C9	177.8(4)	C14-C2-N1-C20	-0.1(4)
C3-C8-C9-C13	-1.7(5)	C3-C2-N1-Ru1	0.8(4)
C7-C8-C9-C13	179.6(3)	C14-C2-N1-Ru1	-179.6(2)
C3-C8-C9-C10	174.3(4)	C19-C20-N1-C2	-178.6(4)
C7-C8-C9-C10	-4.4(6)	C15-C20-N1-C2	0.7(4)
C13-C9-C10-O10	177.2(4)	C19-C20-N1-Ru1	0.7(7)
C8-C9-C10-O10	0.8(7)	C15-C20-N1-Ru1	179.9(3)
C13-C9-C10-N11	-1.5(4)	C6-C5-N4-C3	-1.2(5)
C8-C9-C10-N11	-178.0(4)	C6-C5-N4-Ru1	179.7(3)
C8-C9-C13-C14	0.2(6)	C2-C3-N4-C5	-179.0(3)
C10-C9-C13-C14	-176.5(3)	C8-C3-N4-C5	-0.2(5)
C8-C9-C13-C12	177.8(3)	C2-C3-N4-Ru1	0.4(4)
C10-C9-C13-C12	1.1(4)	C8-C3-N4-Ru1	179.1(3)
O12-C12-C13-C9	-179.4(4)	O12-C12-N11-C10	178.4(4)
N11-C12-C13-C9	-0.3(4)	C13-C12-N11-C10	-0.7(4)
O12-C12-C13-C14	-2.0(7)	O10-C10-N11-C12	-177.4(4)
N11-C12-C13-C14	177.1(4)	C9-C10-N11-C12	1.4(4)
C9-C13-C14-C2	1.7(5)	C23-C22-N21-C26	0.1(5)
C12-C13-C14-C2	-175.3(4)	C23-C22-N21-Ru1	178.2(3)
C9-C13-C14-C15	179.8(4)	C25-C26-N21-C22	-0.6(5)
C12-C13-C14-C15	2.8(8)	C27-C26-N21-C22	176.8(3)
N1-C2-C14-C13	178.2(3)	C25-C26-N21-Ru1	-178.9(3)
C3-C2-C14-C13	-2.3(5)	C27-C26-N21-Ru1	-1.5(4)
N1-C2-C14-C15	-0.5(4)	C26-C27-N28-C29	-175.6(3)
C3-C2-C14-C15	179.0(3)	C26-C27-N28-Ru1	0.5(4)
C13-C14-C15-C16	2.5(8)	C30-C29-N28-C27	47.4(5)
C2-C14-C15-C16	-179.3(4)	C34-C29-N28-C27	-133.2(4)
C13-C14-C15-C20	-177.3(4)	C30-C29-N28-Ru1	-128.1(4)
C2-C14-C15-C20	0.9(4)	C34-C29-N28-Ru1	51.2(5)
C20-C15-C16-C17	1.5(5)	O35-C35-Ru1-N28	12(5)
C14-C15-C16-C17	-178.3(4)	O35-C35-Ru1-N4	106(5)
C15-C16-C17-O17	179.0(3)	O35-C35-Ru1-N1	-173(5)
C15-C16-C17-C18	-0.6(6)	O35-C35-Ru1-N21	1(6)
O17-C17-C18-C19	-179.9(4)	O35-C35-Ru1-C11	-79(5)
C16-C17-C18-C19	-0.3(6)	C27-N28-Ru1-C35	-179.5(3)
C17-C18-C19-C20	0.3(6)	C29-N28-Ru1-C35	-3.9(3)
C18-C19-C20-N1	179.8(3)	C27-N28-Ru1-N4	86.4(3)
C18-C19-C20-C15	0.6(5)	C29-N28-Ru1-N4	-98.0(3)
C16-C15-C20-N1	179.1(3)	C27-N28-Ru1-N1	28.4(7)
C14-C15-C20-N1	-1.0(4)	C29-N28-Ru1-N1	-156.0(5)
C16-C15-C20-C19	-1.5(5)	C27-N28-Ru1-N21	-1.0(3)
C14-C15-C20-C19	178.3(3)	C29-N28-Ru1-N21	174.6(3)
N21-C22-C23-N23	178.8(3)	C27-N28-Ru1-C11	-90.0(3)
N21-C22-C23-C24	-0.3(5)	C29-N28-Ru1-C11	85.6(3)
N23-C23-C24-C25	-178.2(3)	C5-N4-Ru1-C35	-86.2(3)
C22-C23-C24-C25	0.9(5)	C3-N4-Ru1-C35	94.6(3)
C23-C24-C25-C26	-1.4(6)	C5-N4-Ru1-N28	9.3(3)

C3-N4-Ru1-N28	-169.9(2)
C5-N4-Ru1-N1	179.3(3)
C3-N4-Ru1-N1	0.0(2)
C5-N4-Ru1-N21	86.6(3)
C3-N4-Ru1-N21	-92.6(2)
C5-N4-Ru1-Cl1	149.8(8)
C3-N4-Ru1-Cl1	-29.4(11)
C2-N1-Ru1-C35	-93.4(3)
C20-N1-Ru1-C35	87.4(4)
C2-N1-Ru1-N28	58.7(7)
C20-N1-Ru1-N28	-120.5(6)
C2-N1-Ru1-N4	-0.4(2)
C20-N1-Ru1-N4	-179.7(4)
C2-N1-Ru1-N21	87.4(2)
C20-N1-Ru1-N21	-91.8(4)
C2-N1-Ru1-Cl1	176.8(2)
C20-N1-Ru1-Cl1	-2.4(4)
C22-N21-Ru1-C35	-165.4(11)
C26-N21-Ru1-C35	12.7(13)
C22-N21-Ru1-N28	-176.8(3)
C26-N21-Ru1-N28	1.4(2)
C22-N21-Ru1-N4	89.2(3)
C26-N21-Ru1-N4	-92.6(3)
C22-N21-Ru1-N1	8.9(3)
C26-N21-Ru1-N1	-172.9(2)
C22-N21-Ru1-Cl1	-85.7(3)
C26-N21-Ru1-Cl1	92.4(2)

Table S7. Hydrogen bonds for **FL389** [Å and °].

D-H...A	d(D-H)	d(H...A)	d(D...A)	∠(DHA)
N11-H11...O10#1	0.88	2.05	2.894(4)	159.6
O17-H17...O100#2	0.84	1.96	2.790(4)	169.0
N23-H23A...O100	0.80	2.34	3.054(5)	148.1
N23-H23B...Cl1#3	0.89	2.39	3.271(3)	172.5

Symmetry transformations used to generate equivalent atoms:

#1 -x+1,-y+1,-z #2 x+1,y,z #3 -x+2,-y+2,-z+1

A.4.) Resolution of racemic mixtures and determination of absolute configurations

Complex FL172. The enantiomers were separated using a CHIRALPAK IB analytical HPLC column (Daicel/Chiral Technologies, 250 x 4.6 mm) using the solvent of ethanol : hexane (1:1) in 15 minutes with a flow rate of 0.75 ml/minute. The enantiomers were baseline separated under these conditions with retention times of 12.9 (E1) and 15.3 min (E2). The enantiomers do not show any racemization in an ethanol solution over a time period of 12 hours. The CD spectra of the separated enantiomers is shown below in Figure S11 and were recorded on a Model J-810 Spectropolarimeter. The slower eluting enantiomer E2 showed more potent PAK-1 inhibition and was cocrystallized with PAK1 (see part C) and based on this cocrystal structure assigned with the Λ -configuration (For the Λ/Δ -nomenclature, see: *Inorg. Chem.* **1983**, 22, 1569-1573).

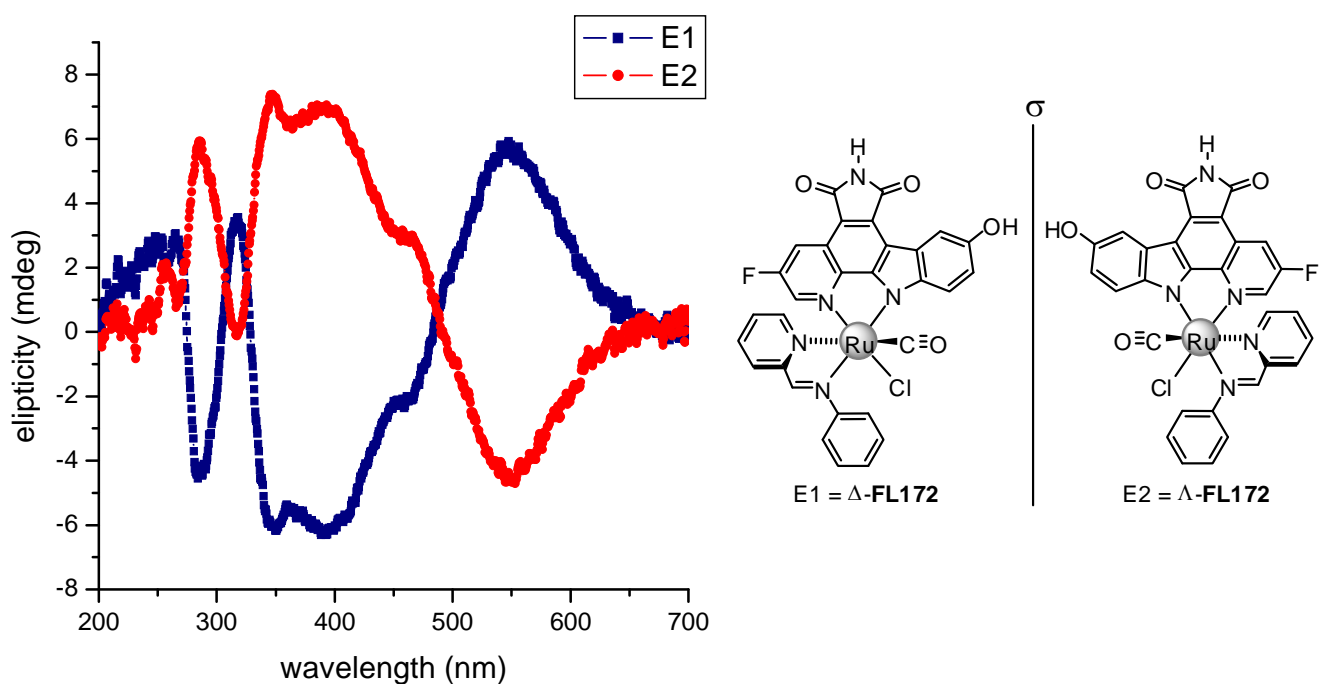


Figure S11. Circular dichroism spectra of the two enantiomers of **FL172**.

Complex FL411: For the resolution of the racemic mixture of **FL411**, the amino group at the 4-position of the pyridine was BOC-protected and removed after the separation with a CHIRALPAK IB analytical HPLC column (Daicel/Chiral Technologies, 250 x 4.6 mm) with the solvent of ethanol : hexane (2:3) in 15 minutes with a flow rate of 0.75 ml/minute. The enantiomers were baseline-separated under these conditions with retention times of ca. 10.5 (E1) and 15.7 min (E2). The enantiomers don't show any significant racemization in an ethanol solution over a time period of 12 hours. The CD spectra of the separated enantiomers after BOC-deprotection is shown below in Figure S12. Absolute configurations were assigned by correlation with the CD spectra of **FL172**.

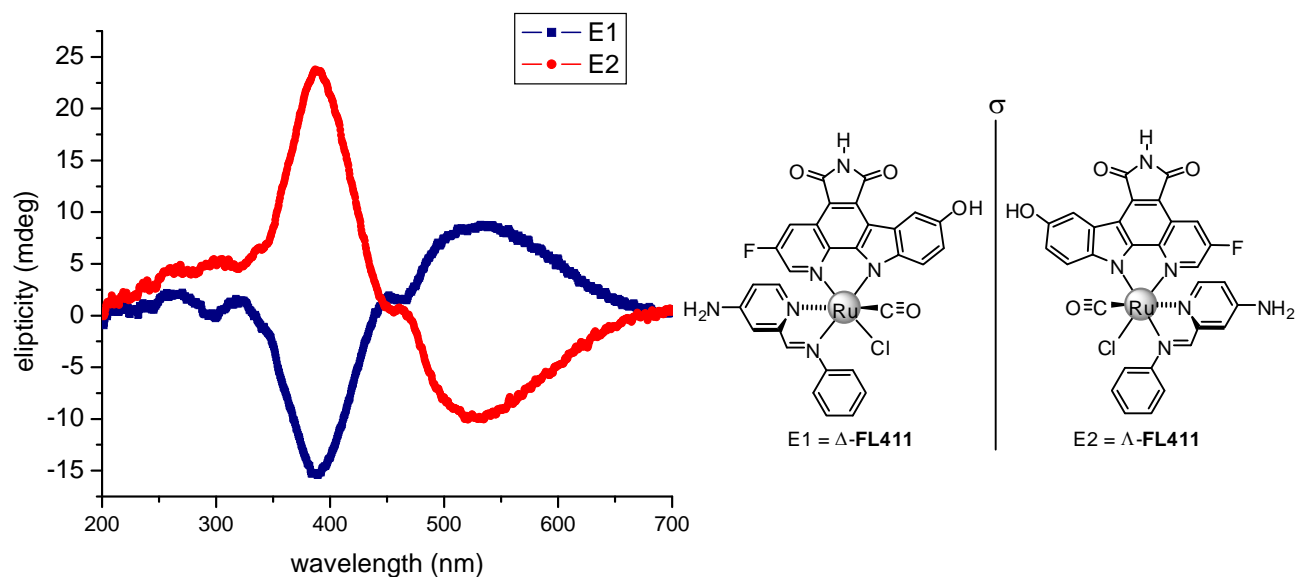


Figure S12. Circular dichroism spectra of the two enantiomers of **FL411**.

B.) Kinase Assays

B.1.) Kinase assays with the protein kinases PAK1, Pim1, and GSK3

PAK1 kinase assay. For in vitro kinase assays, the DNA encoding the kinase domain of PAK1 (residues from 249 to 545) was subcloned into the pFastBac HTc expression vector and protein was expressed in Sf21 cells. Cells were lysed by sonication in 50 mM HEPES pH 7.0, 500mM NaCl and 5 mM DTT (resuspension buffer). The lysate was cleared by centrifugation and applied to a Ni-NTA affinity column. The protein was eluted from the column with increasing concentration of imidazole in resuspension buffer (20 mM to 250 mM) and treated overnight with TEV protease to cleave the His₆-tag. The protein was further purified by passage through Mono-Q and a size-exclusion Superdex 200 column equilibrated with 20 mM Tris pH 8.0, 125 mM NaCl. Purified protein was concentrated to 1.2 mg/ml and frozen for storage.

Kinase assays were performed using labeled γ -P³² ATP and the incorporation of P³²-phosphate into the myelin basic protein (MBP) substrate (Millipore) was monitored. Different concentrations of the inhibitor were incubated with 0.2 nM PAK1 kinase in 20 mM MOPS pH 7.0, 30 mM MgCl₂, 0.8 μ g/ μ L bovine serum albumin and 5% DMSO (resulting from the inhibitor stock solution) in the presence of 25 μ g of MBP substrate for 15 minutes. Reactions were initiated by adding ATP to a final concentration of 1 μ M including 0.2 μ Ci/ μ L γ -³²P ATP in a final volume of 25 μ L. The reactions were terminated by spotting 17.5 μ L onto circular P81 phosphocellulose paper (diameter 2.1 cm, Whatman), followed by washing three times with 0.75% phosphoric acid and one time with acetone. The dried P81 papers were transferred to scintillation vials and 4ml of scintillation cocktail was added. The counts per minute (CPM) were measured in a Packard 1500 Tri-Carb Liquid Scintillation Analyzer and the IC₅₀ values were defined to be the concentration of inhibitor at which the counts per minute (CPM) was 50% of the control sample, corrected for by the background CPM.

Pim1 kinase assay. Kinase assays were performed using labeled γ -P³² ATP and the incorporation of P³²-phosphate into the substrate (S6 kinase/Rsk2 substrate peptide 2) was monitored. Various concentrations of the inhibitor were incubated at room temperature in 20 mM MOPS pH 7.0, 30 mM MgCl₂, 0.8 μ g/ μ l BSA, 5% DMSO (resulting from the inhibitor stock solution), in the presence of substrate (50 μ M) and Pim1 kinase (0.16 nM, except for testing **DW12** and **NP309** where 0.1 nM enzyme was used). After 15 min, the reaction was initiated by adding ATP to a final concentration of 1 μ M, including approximately 0.2 μ Ci/ μ l γ -P³² ATP. Reactions were performed in a total volume of 25 μ L. The reaction was terminated by spotting 17.5 μ L on circular P81 phosphocellulose paper followed by washing four times for five minutes each with 0.75% phosphoric acid and once with acetone. The dried P81 papers were transferred to the scintillation vials, 4 ml of scintillation cocktail were added and the CPM determined with a Packard 1500 Tri-Carb Liquid Scintillation Analyzer. Pim1 kinase and S6 kinase/Rsk2 Substrate Peptide 2 were purchased from Millipore.

GSK3 β kinase assay. The procedure was as described for the Pim1 kinase assay, but in the presence of substrate peptide, Phospho-Glycogen Synthase Peptide-2 (20 μ M), and GSK-3 β (0.2 nM, except for determining IC₅₀ values of **DW12** and **NP309** where 0.1 nM enzyme was used). GSK3 β and the substrate were purchased from Millipore.

Determination of K_m values for ATP. For determination of K_m values of ATP for Pim1, GSK3 β and PAK1, the activity of each kinase was measured under a range of ATP concentrations. Kinase assays were performed as described above. K_m values were calculated using the Michaelis-Menten equation with the GraphPad Prism 5.0 software. All experiments were done in duplicate or triplicate.

	Pim1	GSK3 β	PAK1
K _m -ATP (μ M)	48 \pm 6	9.3 \pm 0.8	4.4 \pm 0.3

B.2.) Selectivity of FL172 in a panel of 264 protein kinases

Kinase	Activity (%)	Kinase	Activity (%)	Kinase	Activity (%)	Kinase	Activity (%)
Abl(h)	94	CHK2(I157T)(h)	67	EphB1(h)	112	Itk(h)	73
Abl(m)	77	CHK2(R145W)(h)	55	EphB3(h)	94	JAK2(h)	117
Abl (H396P) (h)	83	CK1 γ 1(h)	89	EphB4(h)	124	JAK3(h)	92
Abl (M351T)(h)	92	CK1 γ 2(h)	85	ErbB4(h)	93	JNK1 α 1(h)	107
Abl (Q252H) (h)	80	CK1 γ 3(h)	50	FAK(h)	83	JNK2 α 2(h)	100
Abl(T315I)(h)	88	CK1 δ (h)	88	Fer(h)	80	JNK3(h)	68
Abl(Y253F)(h)	88	CK1(y)	59	Fes(h)	127	KDR(h)	39
ACK1(h)	91	CK2(h)	109	FGFR1(h)	96	Lck(h)	61
ALK(h)	117	CK2 α 2(h)	109	FGFR1 (V561M)(h)	49	LIMK1(h)	95
ALK4(h)	0	CLK2(h)	20	FGFR2(h)	108	LKB1(h)	100
Arg(h)	68	CLK3(h)	80	FGFR2 (N549H)(h)	84	LOK(h)	90
AMPK(r)	74	cKit(h)	88	FGFR3(h)	97	Lyn(h)	14
Arg(m)	88	cKit(D816V)(h)	105	FGFR4(h)	89	Lyn(m)	12
ARK5(h)	0	cKit(D816H)(h)	66	Fgr(h)	63	MAPK1(h)	86
ASK1(h)	0	cKit(V560G)(h)	19	Flt1(h)	75	MAPK2(h)	103
Aurora-A(h)	77	cKit(V654A)(h)	94	Flt3(D835Y)(h)	26	MAPK2(m)	99
Axl(h)	50	CSK(h)	110	Flt3(h)	33	MAPKAP-K2(h)	100
Blk(m)	54	c-RAF(h)	44	Flt4(h)	30	MAPKAP-K3(h)	112
Bmx(h)	147	cSRC(h)	59	Fms(h)	28	MEK1(h)	106
BRK(h)	115	DAPK1(h)	104	Fyn(h)	83	MARK1(h)	86
BrSK1(h)	95	DAPK2(h)	90	GCK(h)	99	MELK(h)	23
BrSK2(h)	101	DCAMKL2(h)	80	GRK5(h)	81	Mer(h)	33
BTK(h)	71	DDR2(h)	84	GRK6(h)	75	Met(h)	57
BTK(R28H)(h)	109	DMPK(h)	107	GRK7(h)	25	MINK(h)	95
CaMKI(h)	107	DRAK1(h)	52	GSK3 α (h)	2	MKK4(m)	117
CaMKII β (h)	66	DYRK2(h)	113	GSK3 β (h)	25	MKK6(h)	109
CaMKII γ (h)	50	eEF-2K(h)	112	Haspin(h)	66	MKK7 β (h)	65
CaMKI δ (h)	80	EGFR(h)	94	Hck(h)	30	MLCK(h)	14
CaMKII δ (h)	45	EGFR(L858R)(h)	80	HIPK1(h)	83	MLK1(h)	33
CaMKIV(h)	81	EGFR(L861Q)(h)	94	HIPK2(h)	64	Mnk2(h)	99
CDK1/cyclinB(h)	72	EGFR(T790M)(h)	90	HIPK3(h)	87	MRCK α (h)	111
CDK2/cyclinA(h)	78	EGFR (T790M,L858R)(h)	62	IGF-1R(h)	78	MRCK β (h)	96
CDK2/cyclinE(h)	54	EphA1(h)	97	IGF-1R(h), activated	95	MSK1(h)	48
CDK3/cyclinE(h)	108	EphA2(h)	96	IKK α (h)	123	MSK2(h)	61
CDK5/p25(h)	81	EphA3(h)	109	IKK β (h)	93	MSSK1(h)	100
CDK5/p35(h)	56	EphA4(h)	111	IR(h)	103	MST1(h)	95
CDK7/cyclinH/ MAT1(h)	114	EphA5(h)	119	IR(h), activated	105	MST2(h)	65
CDK9/cyclin T1(h)	96	EphA7(h)	106	IRR(h)	59	MST3(h)	39
CHK1(h)	74	EphA8(h)	118	IRAK1(h)	86	mTOR(h)	87
CHK2(h)	52	EphB2(h)	135	IRAK4(h)	97	mTOR/FKBP12 (h)	100

Kinase	Activity (%)	Kinase	Activity (%)	Kinase	Activity (%)	Kinase	Activity (%)
MuSK(h)	81	PKB α (h)	20	Ret(V804M)(h)	79	SRPK2(h)	85
NEK2(h)	86	PKB β (h)	54	RIPK2(h)	95	STK33(h)	50
NEK3(h)	85	PKB γ (h)	27	ROCK-I(h)	108	Syk(h)	83
NEK6(h)	112	PKC α (h)	63	ROCK-II(h)	83	TAK1(h)	108
NEK7(h)	102	PKC β II(h)	38	ROCK-II(r)	85	TAO1(h)	60
NEK11(h)	49	PKC β III(h)	25	Ron(h)	98	TAO2(h)	37
NLK(h)	98	PKC γ (h)	33	Ros(h)	90	TAO3(h)	65
p70S6K(h)	76	PKC δ (h)	71	Rse(h)	21	TBK1(h)	81
PAK1(h)	17	PKC ϵ (h)	65	Rsk1(h)	13	Tec(h) activated	94
PAK2(h)	26	PKC η (h)	97	Rsk1(r)	22	Tie2(h)	67
PAK3(h)	8	PKC ι (h)	77	Rsk2(h)	33	Tie2(R849W)(h)	61
PAK4(h)	82	PKC μ (h)	102	Rsk3(h)	33	Tie2(Y897S)(h)	82
PAK5(h)	71	PKC θ (h)	15	Rsk4(h)	20	TLK2(h)	100
PAK6(h)	92	PKC ζ (h)	73	SAPK2a(h)	103	TrkA(h)	30
PAR-1Ba(h)	42	PKD2(h)	98	SAPK2a(T106M)(h)	106	TrkB(h)	7
PASK(h)	109	PKG1 α (h)	40	SAPK2b(h)	96	TSSK1(h)	74
PDGFR α (h)	120	PKG1 β (h)	36	SAPK3(h)	112	TSSK2(h)	104
PDGFR α (D842V)(h)	60	Plk1(h)	101	SAPK4(h)	107	Txk(h)	96
PDGFR α (V561D)(h)	51	Plk3(h)	108	SGK(h)	84	ULK2(h)	97
PDGFR β (h)	104	PRAK(h)	48	SGK2(h)	104	ULK3(h)	111
PDK1(h)	92	PRK2(h)	32	SGK3(h)	98	WNK2(h)	77
PhK γ 2(h)	93	PrKX(h)	76	SIK(h)	59	WNK3(h)	81
Pim-1(h)	1	PTK5(h)	68	Snk(h)	99	VRK2(h)	93
Pim-2(h)	1	Pyk2(h)	76	Src(1-530)(h)	60	Yes(h)	54
Pim-3(h)	24	Ret(h)	87	Src(T341M)(h)	73	ZAP-70(h)	126
PKA(h)	69	Ret(V804L)(h)	89	SRPK1(h)	93	ZIPK(h)	108

Measured by Millipore UK Ltd (Millipore Kinase ProfilerTM). PAK1 was measured separately because it was not available in the Kinase Profiler panel. Conditions: 3 μ M **FL172** at an ATP concentration of 10 μ M. Measurements were performed in duplicate and the average taken. Kinases displaying less than 20% activity under these conditions are highlighted.

C.) PAK1 Crystallography

C.1.) PAK1 expression and purification

PAK1 kinase domain (residues 249 to 545, mutation Lys299Arg) was cloned into a pET-TOPO vector with an N-terminal 6-His tag and expressed in BL21(DE3) *E. coli* cells. The kinase domain contained the inactivating mutation Lys299Arg. Cells were grown at 37 °C until they reached an OD₆₀₀ of 0.6 and protein expression was induced by adding 1 mM IPTG for 6 hours at 28°C. Protein was purified from harvested cells as described above. Purified protein was concentrated to 9 mg/ml in a buffer containing 20 mM Tris pH 8.0, 125 mM NaCl, and used for crystallization.

C.2.) Crystallization and data collections

Crystals of apo-PAK1 were obtained using hanging drop vapor diffusion by mixing 1 µL of PAK1 (9 mg/ml) with 1 µL of crystallization solution (0.1 M HEPES pH 7.5, 1 M NaCl, 25% PEG 10000, 10 mM DTT) at 4°C. Crystals were subjected to soaking with 1 mM (*R*)-**DW12** inhibitor overnight. Crystals were cryoprotected, flash frozen in liquid nitrogen and yielded X-ray diffraction to 2.35 Å at the APS 23 ID-B beam line.

For structure determination of PAK1 in complex with **Λ-FL172**, PAK1 was cocrystallized with octahedral ruthenium complex. **Λ-FL172** was added to protein from 10 mM stock solution in DMSO to the final concentration of 1 mM and incubated on ice for 1 hour. Crystals were grown at 4 °C in 2 µl drops where 1 µl of protein/inhibitor solution was mixed with 1 µL of precipitate stock containing 0.1M Tris pH 8.0, 1M NaCl, 25% PEG 4000, 10 mM DTT. Cryoprotected crystals were flash frozen in liquid nitrogen and yielded X-ray diffraction to 1.65 Å at the APS 23ID-B beam line. For both structures, data were integrated and scaled using HKL2000 (Z. Otwinowski, W. Minor, *Methods Enzymol.* **1997**, 276, 307-326).

C.3.) Structure determination and refinement

PAK1 inhibitor complex structures were solved by molecular replacement using the program Phaser (A. J. McCoy, R. W. Grosse-Kunstleve, L. C. Storoni, R. J. Read, *Acta Cryst.* **2005**, *D61*, 458-464) with the unliganded PAK1 (249-545, Lys299Arg) structure (PDB code 1YHW) as a search model (M. Lei, M.A. Robinson, S. C. Harrison, *Structure* **2005**, *13*, 769-778). Iterative cycles of refinement and manual rebuilding of the initial model were performed using the programs REFMAC5 (G. N. Murshudov, A. A. Vagin, E. J. Dodson, *Acta Crystallogr. Sect. D* **1997**, *53*, 240-255) and COOT (P. Emsley, K. Cowtan, *Acta Crystallogr. Sect. D: Biol. Crystallogr.* **2004**, *60*, 2126-2132), respectively. Inhibitor models were manually fitted into calculated F_o - F_c maps (Figure S13). The validity of each step of refinement and rebuilding was monitored by the R_{work} and R_{free} .

In both structures, after further refinement, both $2F_o$ - F_c and F_o - F_c electron density maps showed clear and positive density for a phosphate group on Thr423 of the activation loop (Figure S14). Phosphorylation of Thr423 is known to stabilize the active conformation of the enzyme and the activation loop in both complexes adopts a conformation typical for the active kinase. The conformation of the activation loop is the same as in previously published structures: PAK1(K299R) and the PAK1 double mutant (K299R, T423E) (M. Lei, M.A. Robinson, S. C. Harrison, *Structure* **2005**, *13*, 769-778). The T423E mutation generates constitutively active enzyme when lysine is present at position 299, mimicking salt bridges between phosphothreonine and Arg388 and Arg421 that are present in our structures (Figure S14). The identical positions of the activation loop residues in our structures with previously published structures and the presence of phosphothreonine confirms that PAK1 in complex with both (*R*)-**DW12** and Δ -**FL172** adopts an active conformation. Data collection and refinement statistics for both complexes are shown in Table S8.

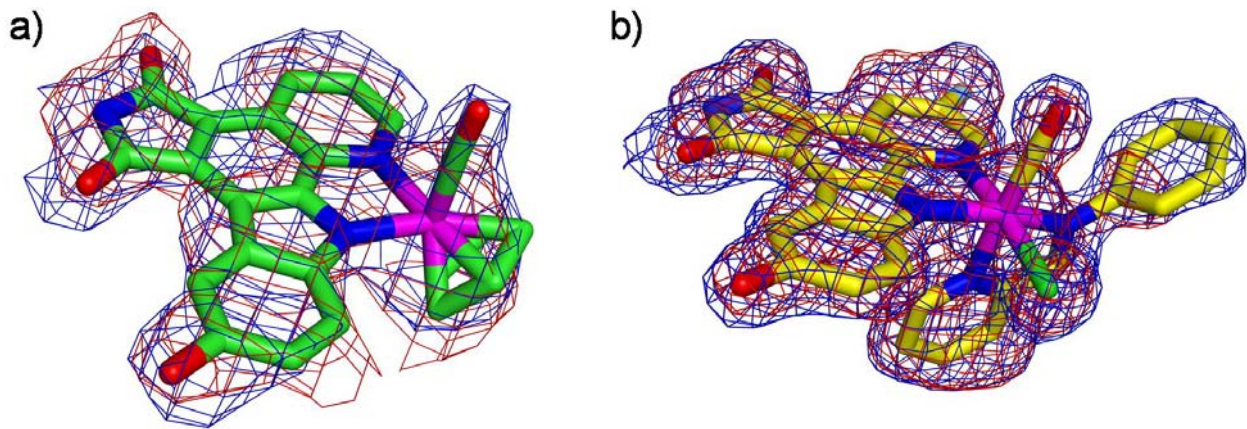


Figure S13: Electron density corresponding to **(R)-DW12** (a) and **Λ-FL172** (b). Fo-Fc electron density maps shown in red contoured at 2.5σ calculated before building the inhibitor models, 2Fo-Fc electron density maps in blue, contoured at 1σ after refining the structures with bound inhibitors.

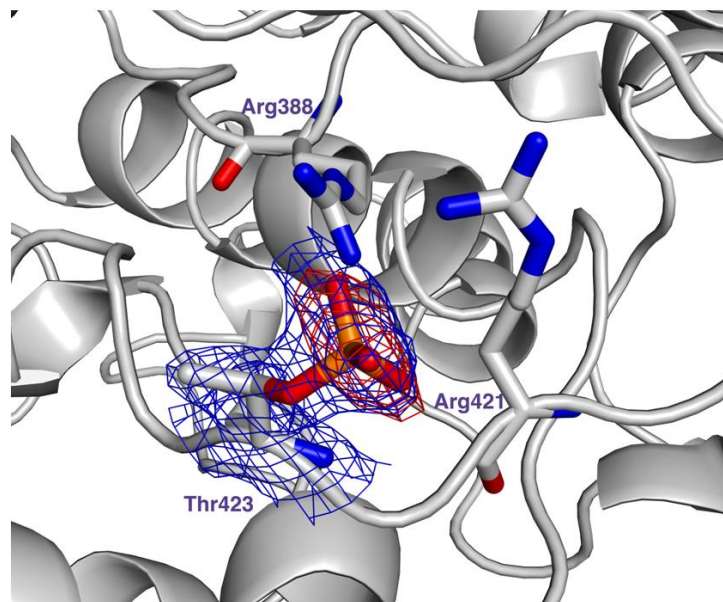


Figure S14. Phosphorylated Thr423, Arg388 and Arg421 shown only for PAK1-**Λ-FL172** complex, since positions of corresponding residues in complex with **(R)-DW12** are virtually identical. In blue 2Fo-Fc electron density map for phospho-Thr contoured at 1σ , in red Fo-Fc electron density contoured at 2.5σ calculated before refinement with the phosphate group modeled.

Table S8. Data collection and refinement statistics.

<i>Data collection</i>		
Complex	PAK1-(R)-DW12	PAK1-Δ-FL172
Space group	C222 ₁	C222 ₁
Cell dimensions [Å, °]	a=53.050 b=102.66 c=122.341 α=β=γ=90	a=52.183 b=103.475 c=122.653 α=β=γ=90
Resolution [Å]	50.0- 2.35	30.0- 1.65
Reflections total, unique	78429, 14162	267916, 40150
R _{merge} ^a	0.143 (0.402)	0.077 (0.53)
I/σ	11.3 (4.0)	22.5 (3.0)
Completeness [%]	99.2 (100)	98.7 (94.1)
Redundancy	5.5 (5.6)	6.7 (5.9)
<i>Refinement</i>		
R _{work} /R _{free} [%]	20.2/ 26.0	19.5/ 21.8
Ramachandran [%] favoured / allowed / disallowed	90.0/ 10.0/ 0	91.9/ 8.1/ 0
R.m.s.d. ^b Bond lengths [Å] Bond angles [°]	0.012 1.321	0.011 1.339

^a Data for highest resolution shell in parentheses^bR.m.s.d = root-mean-square-deviation

D.) Cell-Based Assays

Cell culture conditions: RT4 rat schwannoma cells were grown in low-glucose DME, 10% fetal calf serum, 1x non-essential amino acids and 100 IU/ml penicillin-streptomycin. For the treatment with racemic **FL172**, cells were first serum-starved overnight and then incubated for 1 hour with the compound at the final concentration ranging of 0.5 -20 µM. DMSO was used as negative control.

Kinase assay: Following **FL172** treatment, RT4 cells were stimulated with 10 ng/ml PDGF for 5 minutes and then lysed in cell lysis buffer (40 mM HEPES, pH 7.4, 1% NP-40, 100 mM NaCl, 25 mM NaF, 1 mM EDTA, 1mM Na₃VO₄ and 1x protease inhibitor cocktail). Protein concentration in cell extracts was determined using the Bradford assay and 500 µg of the cell extracts were immunoprecipitated with Pak1 antibody-coupled beads (Santa Cruz). The beads were then washed 5 times with lysis buffer and twice with kinase buffer (40 mM HEPES, pH 7.4, 10 mM MgCl₂). For the kinase reaction, 20 µl of kinase reaction mix (4 µg Histone H4, 20 µM cold ATP, and 10 Ci [³²P]γATP in kinase buffer) was added to the beads and incubated at 30 °C for 10 min. The reaction was terminated by adding protein sample buffer and boiling for 5 min. The samples were then resolved by SDS-PAGE and exposed to film (Figure S15).

Western blot: The aliquots of the obtained cell extracts were resolved by SDS-PAGE and transferred to a PVDF membrane. Each sample contained the same amount of protein as determined by the Bradford assay. After the transfer, membranes were probed with the following antibodies: pRaf-1(S338) (Cell Signaling), pMEK(S298) (Millipore), pMEK(S217/221) (Cell Signaling), MEK (Cell Signaling), Pak1 (N-20, Santa Cruz), α-tubulin (AC42, Sigma), according to manufacturer's instructions (Figure S15). Data for phospho-Raf-1(Ser338) and total Raf-1 (antibody from Cell Signaling) were generated probing the cell lysate obtained in the same way as described in an independent experiment (Figure S16).

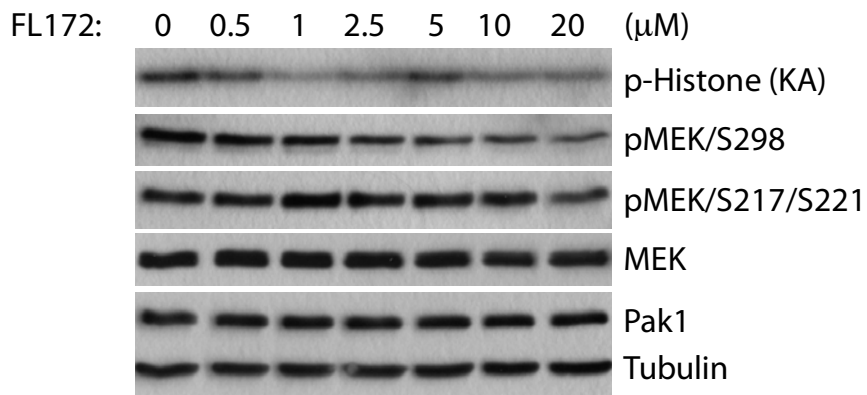


Figure S15. Serum-starved RT4 rat schwannoma cells were treated with racemic **FL172** at indicated concentrations for 1 hour and then stimulated with 10ng/ml PDGF for 5 minutes. Cell extracts were prepared from these cells and immunoprecipitated with PAK1 antibody-coupled beads. An *in vitro* kinase assay (KA) was carried out with the immunoprecipitates using Histone H4 as the substrate. Western blot analysis was also performed using aliquots of the extracts with various antibodies as indicated.

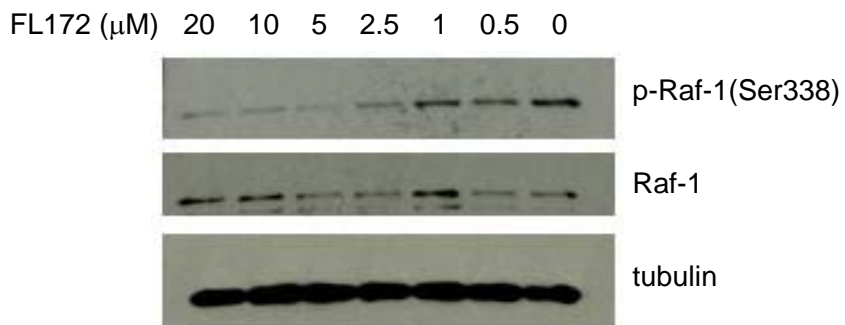


Figure S16. Serum-starved RT4 cells were treated with **FL172** at indicated concentrations for 1 hour and then stimulated with 10 ng/ml PDGF for 5 min. PAK1 inhibition was monitored by levels of Ser338-phosphorylated Raf-1 analyzed by Western blot with an anti-phospho-Raf-1(Ser338). Antibodies against endogenous levels of total Raf-1 and tubulin served as controls.